The Mechanistic Diversity of the Thermal and Photochemical Decomposition of Bis(phenylphosphonoyl)Peroxides: Concerted Polar, Homolytic, and Electron-Transfer Processes
On the Reactivity of (Phenylphosphonoyl)oxyl Radicals

Hans-Gert Korth* and Petra Lommes

Institut für Organische Chemie, Universität-GH Essen,
Universitätsstraße 5, W-4300 Essen 1, F.R.G.

Received March 6, 1992

Key Words: Oxyl radicals / Phosphonoyl peroxides / Laser flash photolysis / ESR-Spin trapping / Electron transfer

The thermal and photochemical decomposition of the first bis(phenylphosphonoyl)peroxides, dioxybis[(*n*-butoxy)phenylphosphane oxide] (**5**), and dioxybis[(phenoxy)phenylphosphane oxide] (**6**) has been studied in various solvents by ^{1}H-, ^{13}C-, and ^{31}P-NMR spectroscopy, laser flash photolysis (LFP), and ESR spin-trapping experiments. Kinetic studies reveal at 20°C a ca. 270 times slower thermal decay for **5** than for **6**, which primarily results from a lower *A* factor rather than differences in the activation energies. The thermal decay of **5** occurs predominantly by a novel, presumably concerted polar rearrangement with formation of a thermally unstable, mixed phosphonoyl-phosphoryl anhydride. Photolysis of **5** induces homolytical cleavage of the peroxy bond with release of [(*n*-butoxy)phenylphosphonoyl]oxyl radicals **7**. Radical **7** is characterized by a broad, transient UV/Vis absorption spectrum in the 400 to >700 nm range (λ_{max} ca. 580 nm), as has been demonstrated by 248-nm LFP of **5** in acetonitrile solution. The short lifetime of this absorption indicates an extremely high reactivity (in hydrogen abstraction and addition) of this electrophilic radical. The thermal and photochemical decomposition of peroxide **6** leads to a virtually identical product distribution, suggesting O–O bond cleavage to be the major initial reaction under both conditions. LFP at 248 and 308 nm of a solution of **6** in acetonitrile initially produces a weak, broad absorption at ca. 500 nm and stronger bands at 280 and 400 nm. The highly transient 500-nm absorption is assigned to the [(phenoxy)phenylphosphonoyl]oxyl radical **8**, the other bands are attributed to the phosphonoyloxy-substituted benzene radical cation **8Z**. The formation of this species can be explained in terms of electron transfer in the first-formed oxyl radical **8** and/or the intact peroxide **6**, followed by cleavage of the peroxy bond. The decay of **8Z** is accompanied by the build-up of the absorption spectrum of a 1,4-dioxy-substituted biphenyl radical cation.

The high reactivity of transient, oxygen-centered radicals of the general structure $Y_nX(O)_mO^{\bullet}$ (**1**), such as carbonyloxyl radicals [$R(CO)O^{\bullet}$; R = Ar, OR′, R′CH=CH, R′C≡C][1], phosphinoyloxyl radicals [$R_2P(CO)O^{\bullet}$; R = Ph][2], and sulfonyloxyl radicals [$RS(O)_2O^{\bullet}$, R = Me, 3-$CF_3C_6H_4$][3] towards organic substrates (hydrogen abstraction and addition) has been interpreted in terms of their very strong electrophilic character, which arises from the contribution made to the radical's ground state by the charge-separated canonical structures **1**.

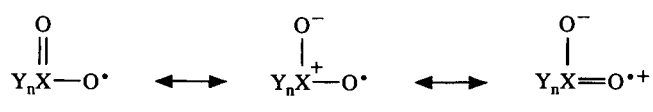

1

All classes of the above radicals are characterized by broad optical absorptions in the visible region. Differences in the reactivity of different $Y_nX(O)_mO^{\bullet}$, as measured by laser flash photolysis (LFP)[1–3], have been attributed to variations in the relative contribution that polar, canonical structures, e.g. $[Y_nX(O)_mO^{-},RH^{+\bullet}]^{\ddagger}$, make to the stabilization of the transition state for hydrogen-atom abstraction or addition reactions[1,2]. In agreement with this hypothesis, we have found that the (diphenylphosphinoyl)oxyl radical, $Ph_2P(O)O^{\bullet}$ (**2**)[2], and sulfonyloxyl radicals[3] are the most reactive "organic" oxygen-centered radicals yet reported. Only the hydroxyl radical exhibits a comparable or slightly higher reactivity[3].

With regard to the above, we hypothesized that it might be possible to modify the reactivity within the phosphorus-centered series $Y_nP(O)O^{\bullet}$ by successive replacement of the phenyl groups in **2** by oxygen substituents, i.e. alkoxy or

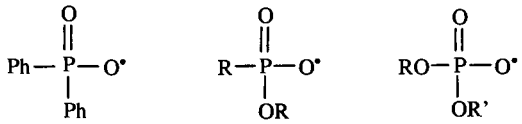

2 **3** **4**

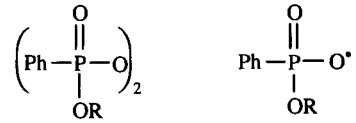

5: R = *n*Bu
6: R = Ph

7: R = *n*Bu
8: R = Ph

  0009–2940/92/1111–2419 $ 3.50+.25/0

aryloxy groups. This hypothesis is based on the view that the π electron-donating ability of the oxygen substituent(s) might partially compensate for the high electron deficiency at the central phosphorus atom, thus decreasing the electrophilicity of the radicals, or, if the σ acceptor property (electronegativity) of the oxygen substituent is of more importance than the π-donating effect, an unchanged or even increased reactivity could be expected. Therefore, we intented to detect the transient electronic spectra of radicals **3** and **4** and then, hopefully, to measure the kinetics of their reactions with organic substrates using laser flash photolysis (LFP).

For LFP purposes the most suitable precursors of **3** and **4** are the symmetrical bis(phosphorus) peroxides $[RP(O)(OR')O]_2$ and $[(R'O)_2P(O)O]_2$, respectively. However, in contrast to the vast number of their carbon-centered counterparts, the diacyl peroxides, phosphorus peroxides of that kind are exceedingly rare[4]. Only one paper[5] could be found in the literature in which the synthesis of peroxides of these types (R = alkyl) has been described, however, they were not very well characterized. Here we report on the synthesis of the first bis(phosphonoyl) peroxides, dioxybis-[(*n*-butoxy)phenylphosphane oxide] (**5**) and dioxybis-[(phenoxy)phenylphosphane oxide] (**6**), their thermal and photochemical decomposition, and the generation and characterization by NMR, ESR, and LFP of the corresponding (phenylphosphonoyl)oxyl radicals **7** and **8**.

Results

Synthesis and Characterization of 5 and 6

A number of different (standard) procedures[4] and variations of the reaction conditions were tested for the preparation of these peroxides, starting from the readily available acyl chlorides **9**, **10**[6]. The formation of **5** and **6**, as followed by ^{31}P-NMR spectroscopy, turned out to be extremely sensitive to the reaction conditions. The procedures described in the experimental part were found to give the best results, though the yields (8–47%) are still fairly low. Only minor variations in the reaction conditions, e.g. temperature, reaction time etc., dramatically decreased the yields. Byproducts were the corresponding phenylphosphonic acid monoesters **11**, **12**, the phenylphosphonic acid diesters **13**, **14**, and the diphenyldiphosphonic acid diesters **15**, **16**.

The structure of compounds **5** and **6** was elucidated by several physical methods. In the ^{31}P-NMR spectra of both peroxides two peaks (**5**: δ = 21.4 and 21.2, **6**: 25.0 and 24.8; in $CDCl_3$) were detected in the chemical shift region expected for this class of compounds[7]. The relative intensity ratio of the two peaks varied somewhat for products obtained from different synthetic runs. Since the elemental analyses of carefully purified products gave satisfying C and H percentages, the two peaks in the ^{31}P-NMR spectrum are attributed to the *meso*- and D,L-diastereomers of **5** and **6**.

The presence of *meso*- and D,L-diastereomers was further corroborated by the ^{13}C-NMR spectra. The spectra revealed the presence of two species having virtually identical spectra but exhibiting slightly different chemical shifts for corresponding resonances. The intensity ratio of corresponding peaks agreed well with the ratio of the two resonances in the ^{31}P-NMR spectrum. The apparent triplet and quintet splittings of some resonances can be explained by the presence of an AXX' (A = ^{13}C, X,X' = P) system in which the two phosphorus atoms couple to each other. Similar splitting patterns have been observed in organometallic diphosphane complexes[8]. The assignment of the carbon resonances is based on a comparison with the ^{13}C-NMR data of related compounds (see Experimental) and literature data[9]. Because of their complexity the ^{1}H-NMR spectra were less useful for the elucidation of the structures of **5** and **6**. However, for **6** (and also products deriving from it) they did at least allow a reasonably good estimate of the ratio of the numbers of hydrogens on phosphorus-bound phenyl groups (δ = 7.3–8.0) to the number on oxygen-bound phenyl groups (δ = 7.0–7.3).

Product Studies

Thermal Decomposition of 5

The kinetics of the thermal decomposition of the peroxides was determined by following the decay of their ^{31}P-NMR signals. In the temperature range from 62 to 79 °C the decay of **5** in $CDCl_3$ (0.3 M) followed a first-order rate law with a rate constant of $k^{333\,K} = 4.3 \cdot 10^{-6}\ s^{-1}$ at 60 °C. From the activation parameters (Table 1) a half-life of 108 d at 25 °C was calculated. The decay rate was almost the same in CCl_4 ($k^{333\,K} = 3.7 \cdot 10^{-6}\ s^{-1}$) but ca. 4 times higher in CD_3CN ($k^{333\,K} = 1.4 \cdot 10^{-5}\ s^{-1}$) (see Table 3).

The decay of the signals of peroxide **5** (containing some **13** and **15**; Figure 1a) was initially accompanied by the growth, with the same rate, of signals at δ = 10.8 and −18.0, respectively, (Figure 1b) typical values for compounds incorporating both a phosphonyl and a phosphoryl group[7]. The spectral pattern implied the presence of two diastereomers, having identical P,P splittings J_{pp} = 26.7 Hz. In fact, we identified these signals to be due to the mixed phosphonic phosphoric anhydride **17** by "spiking" with independently synthesized material.

Compound **17** itself appeared to be thermally unstable; it further decayed with a half-life of $t_{1/2}$ = 126.3 h at 62 °C to

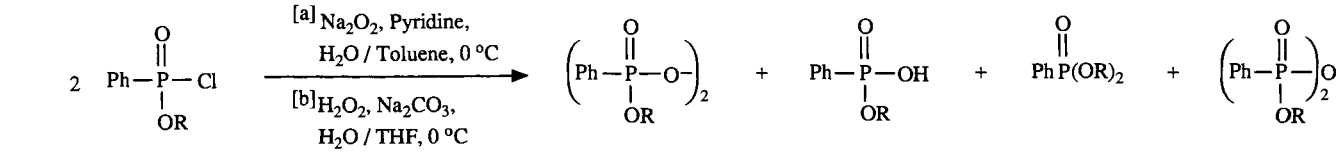

[a] R = *n*Bu: **9** **5** **11** **13** **15**

[b] R = Ph: **10** **6** **12** **14** **16**

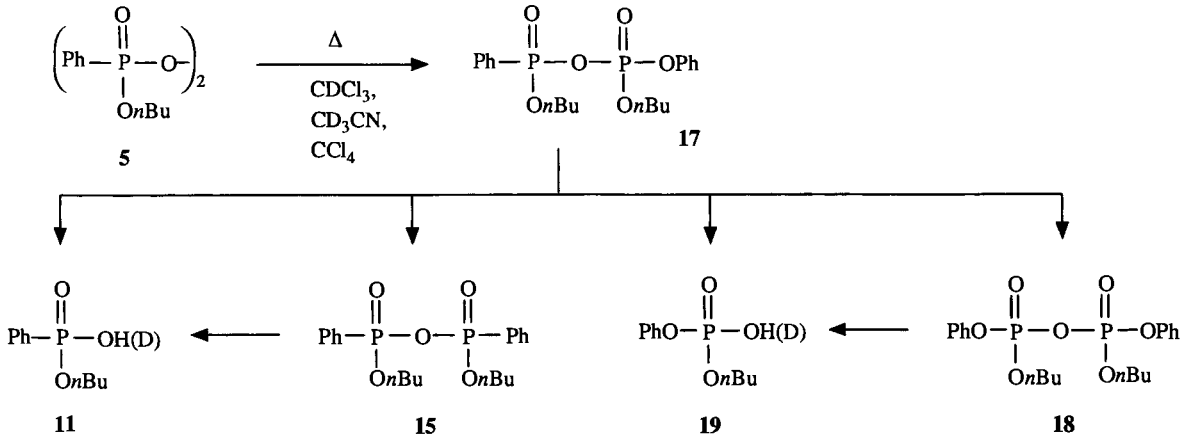

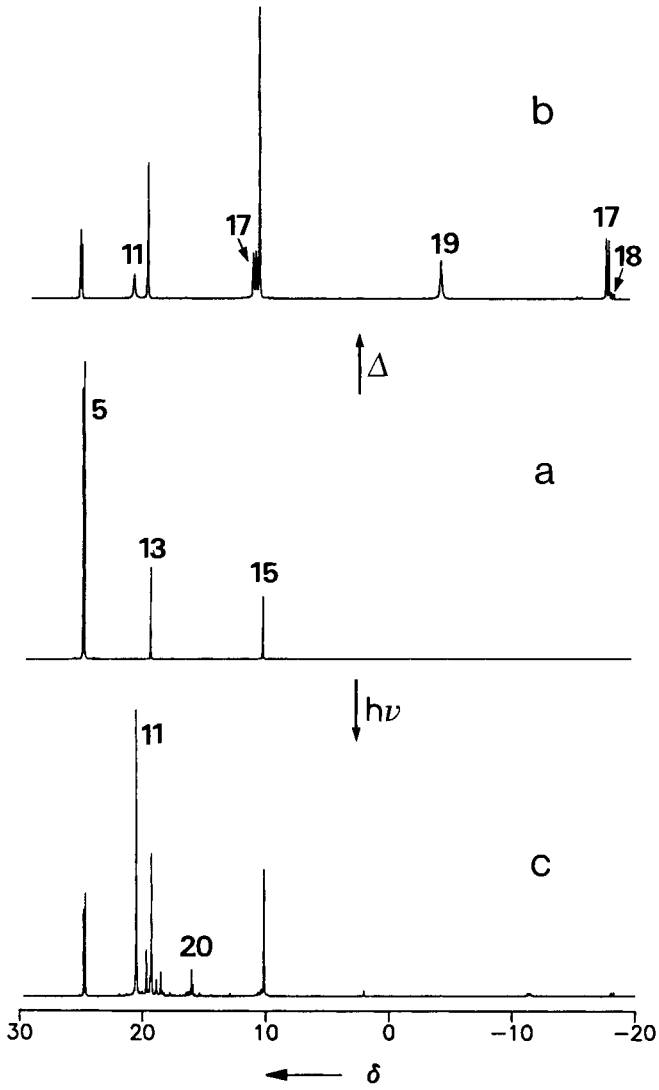

Fig. 1. ^{31}P-NMR spectra ($CDCl_3$) of 0.2 M solutions of peroxide **5**, (a) before, (b) after thermal (62°C; 94 h), and (c) after photolytical (20°C; 30 min) decomposition

produce the monoester **11** (δ = 20.5), the phosphonic anhydride **15** (δ = 10.4 and 10.3), the phosphoric anhydride **18** (δ = −18.3 and −18.5), and the phosphoric acid diester **19** (δ = −4.5) (Table 4).

Table 1. Activation parameters for the thermal decomposition of peroxides **5**, **6**, and **40** in $CDCl_3$

Peroxide	E_A [kcal mol^{-1}]	lg A/s^{-1}	r^{2}[a]	k^{298} [s^{-1}][b]
5	22.5±1.3	9.4±0.8	0.993	$7.4 \cdot 10^{-8}$
6	21.4±1.7	11.0±1.3	0.987	$2.0 \cdot 10^{-5}$
40[c]	21.7±1.1	11.8±0.8	0.998	$7.6 \cdot 10^{-5}$

[a] Measure of determination for least-squares fit. — [b] Calculated from the Arrhenius parameters. — [c] From rate data in ref.[24] and own measurement at 21.5°C.

No significant changes in the product distributions were observed when **5** was decomposed in CCl_4 or CD_3CN solution (see Table 4). Also, the original percentage of **13** was not affected. The time evolution of the secondary products implied that most of **11** and **19** was not directly formed from **17** but largely derived from a further reaction of **15** and **18**, respectively. In agreement, the signals of the latter compounds disappeared completely when the sample was kept at room temperature for several weeks, leaving only the signals of **11**, **19**, and **13**. Presumably, the further decay of **15** and **18** is just a hydrolysis reaction, since it proved very difficult to remove traces of water from the starting peroxide **5**, and no special care was taken to exclude air. Particularly **18** seems to be fairly unstable under the applied conditions. However, a small part of **11** is likely to be formed by a direct, nucleophilic attack of water on the peroxide **5**[10]. This was indicated by the time evolution of the relative percentage of **11**, for which after an initial rapid increase an intermediate decrease was observed.

Photochemical Decomposition of 5

The photochemically initiated decomposition of peroxide **5** led to an entirely different product spectrum than its thermal decay. UV photolysis (λ < 360 nm) at 20°C in $CDCl_3$, CCl_4, or CD_3CN solution (0.1−0.3 M) caused an almost complete destruction of **5** within one hour. In all cases, acid **11** appeared to be by far the major product, accompanied by a varying number ($\geq$6) of minor products (Figure 1c; see Table 5), most of which exhibited ^{31}P-NMR resonances in the region of δ = 15−20. Anhydride **17**, the primary product of the thermal process, could be detected in traces only.

Also, neither **19** nor additional **15** were formed. Thus, the photochemical decomposition obviously follows a different route than the thermal process. The high yield of **11** strongly suggested the homolytic cleavage of the peroxy bond with release of free [(*n*-butoxy)phenylphosphonoyl]oxyl radicals **7**. These (expectedly highly reactive) radicals then decayed by hydrogen abstraction from the solvent and the parent peroxide and/or addition to the latter.

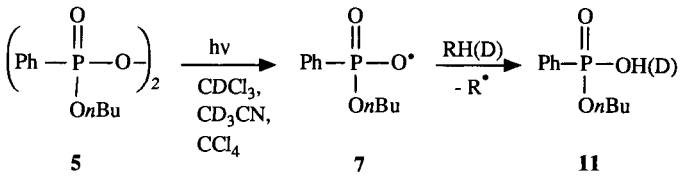

5 **7** **11**

Since all of the minor reaction products were produced in <10% of the total sum of products, we made no effort to identify them individually. The ^{31}P-, ^{13}C-, and ^{1}H-NMR spectra of the reaction mixtures indicated that the side products were mainly various phenylphosphonic acids and esters. Hydrogen abstraction followed by radical coupling and radical-induced decomposition of **5** easily explains their formation. Hydrogen abstraction from the *n*-butyl group – an intramolecular process should be entropically favored for radical **7** – was clearly indicated by detection of several (≥12) new CH_2 and CH resonances in the range of δ = 20–70 in the ^{13}C-NMR spectra, as expected for products deriving from coupling of the various possible *n*-butyl-type radicals. Substitution (branching) in the C-2-to-C-4 positions of the *n*-butyl group should not have a significant effect on the ^{31}P-NMR shift of **11**, so the peak assigned to this compound is likely to incorporate some percentage of various phenylphosphonic acid esters carrying substituted butyl groups. The high complexity of the ^{13}C- and ^{1}H-NMR spectra prohibited a more detailed assignment. Attack on the solvents (preferably by **7**) seems to be of minor importance (particularly for CD_3CN) since only small amounts of perdeuterated succinonitrile [$(CD_2CN)_2$] and $CHCl_3$ were detected after decomposition in CD_3CN and $CDCl_3$ solution, respectively. The only byproduct which we unequivocally identified was phenylphosphonic acid *n*-butyl phenyl ester (**20**) [^{31}P NMR ($CDCl_3$): δ = 16.2]. This compound, the relative yield of which was more or less the same in all three solvents can be reasonably explained to derive from *ipso* attack of radical **7** on the phenyl group of its precursor.

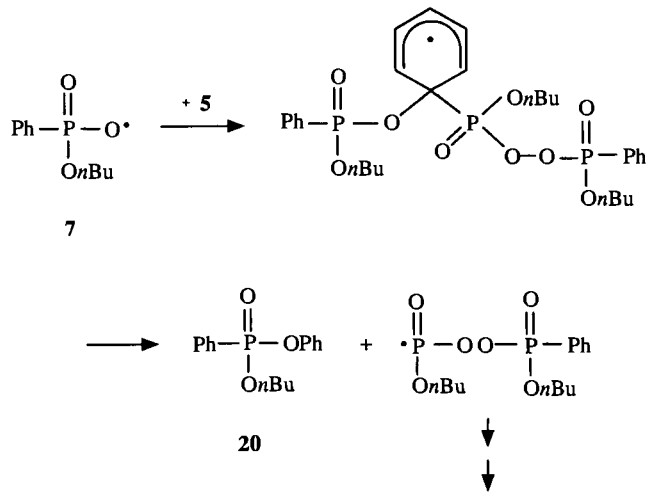

7

20

When peroxide **5** was photodecomposed in CCl_4 solutions containing a tenfold excess of the hydrogen donors cyclohexane or 1,4-cyclohexadiene the yield of **11** (93 and 82%, respectively) was increased and less side-products were formed (Table 5), as expected for a free-radical decay mechanism.

Thermal Decomposition of 6

The thermal decomposition of **6** (0.05–0.06 M) in $CDCl_3$, CD_3CN, or benzene solution occurred much faster than that of **5**. In the temperature range from 15 to 33°C the decay in $CDCl_3$ followed a first-order rate law with a rate constant of $k^{298\,K} = 2.0 \cdot 10^{-5}\ s^{-1}$ at 25°C. In CD_3CN the decomposition was accelerated by approximately a factor of two. The Arrhenius parameters (Table 1) reveal that the ca. 270 times increased decay rate compared to **5** arises primarily from the higher *A* factor rather than from a considerable difference in the activation energies.

At room temperature all solutions of **6** turned yellow within ca. 20 min, and a brownish precipitate was formed after several hours. The precipitate accounted for 7–24% of the mass of the starting peroxide **6** for various experiments. After separation, the solutions and precipitates (which could be dissolved in [D_6]DMSO) were analyzed by ^{1}H-, ^{13}C-, and ^{31}P-NMR spectroscopy. Very similar product distributions were found for the three solvents. In the ^{31}P-NMR spectra of the clearified solutions several new peaks were detected in the range of δ = 5–20 (Figure 2; Table 6). The most intense peak (δ = 17.8 ± 0.6; $CDCl_3$) was identified as that of phenylphosphonic acid phenyl ester (**12**)[11]. The high yield of **12** (57–75%) is most reasonably interpreted in terms of a homolytic O–O cleavage of the peroxide **6** to give radical **8**, followed by hydrogen (deuterium) abstraction from the solvent and/or some reaction products.

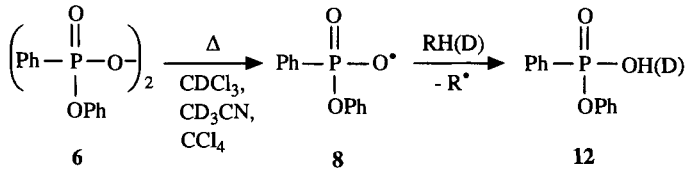

6 **8** **12**

The assignment of most of the minor peaks in the ^{31}P-NMR spectra indicated products of structural similarity to **12**. Accordingly, the peak at δ = 16.6 was identified as being due to phenylphosphonic acid (**21**) (5–15%). Diphosphonic acid diphenyl ester **16** (δ = 6.2)[12] as well as an unidentified product with δ = 9.7 were formed only after prolonged reaction times, thus, their formation is likely to be the result of further reactions of the primary decomposition products. The corresponding ^{13}C-NMR spectra were fully consistent with the above assignments, showing that the peaks in the region of δ = 16–18 of the ^{31}P-NMR spectra represent the

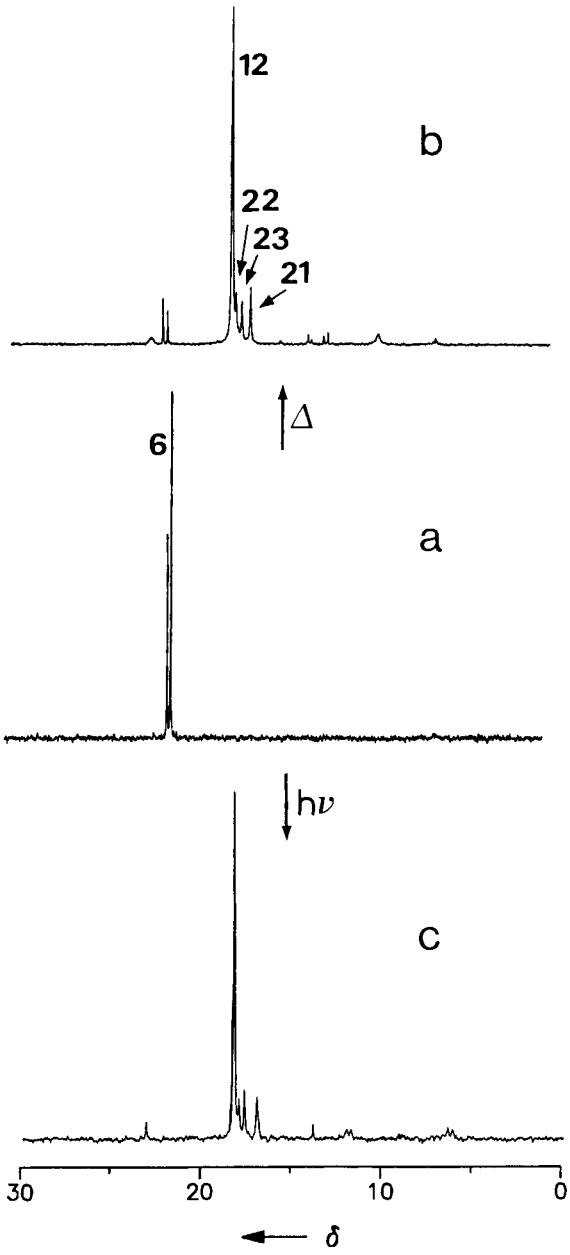

Fig. 2. ^{31}P-NMR spectra ($CDCl_3$) of 0.07 M solutions of peroxide **6**, (a) before, (b) after thermal (30°C; 28 h), and (c) after photolytical (20°C; 20 min) decomposition

soluble portions of the compounds which formed the precipitates (see below).

The [D_6]DMSO solutions of the precipitates showed four major peaks between δ = 13 and 14 in the ^{31}P-NMR spectrum (Table 6), two of which were due to compounds **12** and **21**. Since the other two peaks exhibited similar strong shifts of their ^{31}P-NMR resonances on changing the solvent from $CDCl_3$ to [D_6]DMSO, we suspected that they also respresented compounds incorporating the phenylphosphonic acid moiety [PhP(O)OH]. Elaborate analysis of the ^{13}C- and ^{1}H-NMR spectra led to the conclusion that the dimeric phenylphosphonic acid **22** (7–15%) could be one of the components. This was unequivocally confirmed by independent synthesis and "spiking" of the NMR resonances. Thus, formally a coupling of two phenylphosphonic acid phenyl ester moieties in the *para*-positions of the phenoxyl groups had occurred during the decomposition of **6**. The remaining ^{31}P-NMR peak from the precipitate was tentatively attributed to an isomer of **22**, the bis(phenylphosphonic acid) **23** (5–15%), as suggested by the ^{13}C-NMR spectrum of the reaction mixture.

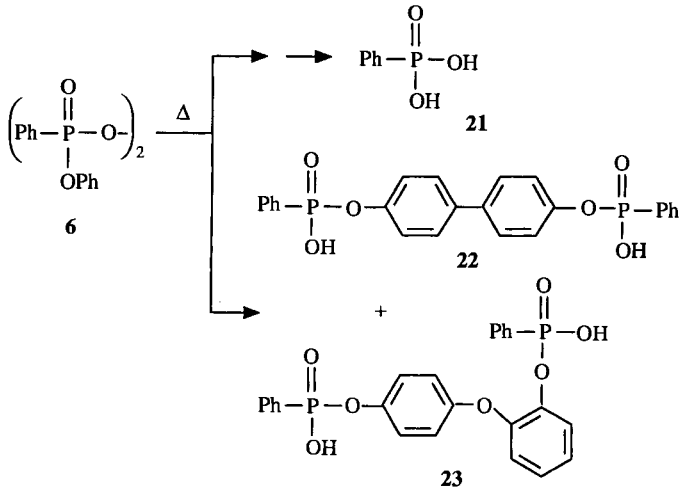

In order to gain additional support for a free-radical decay mechanism, peroxide **6** was also decomposed in the presence of some compounds which are known to react rapidly (by hydrogen abstraction and/or addition) with electrophilic oxygen-centered radicals[1–3]. For instance, decomposition of **6** in CD_3CN at 22°C in the presence of excess 1,4-cyclohexadiene gave acid **12** in high yield (80%). In this case the solution remained colorless, and no insoluble products were formed. With added triethylsilane the decay of **6** in CD_3CN was slightly accelerated, producing **12** (ca. 51%) and the triethylsilyl ester **24** (23%) as the major products. The relatively high yield of **24** is unlikely to derive entirely from recombination of radical **8** and triethylsilyl radicals. Since

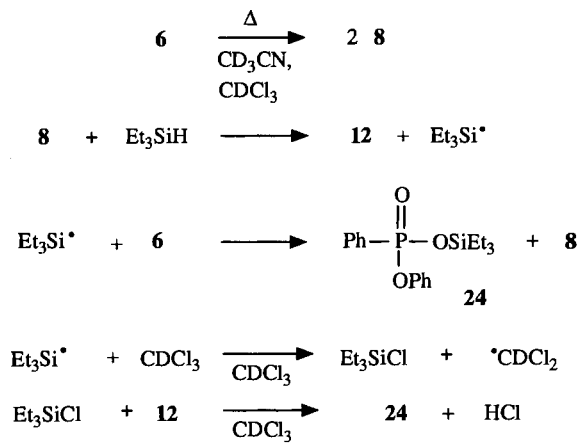

acid **12** does not react thermally with triethylsilane under these conditions, the considerable amount of **24** implies an induced decomposition of peroxide **6** by triethylsilyl radicals. The formation of other compounds, *viz.* **21**–**23**, was suppressed beyond the detection limit (< 3%). The silyl ester **24** became the main product (70%) when $CDCl_3$ was used as a solvent for the decomposition of **6** in the presence of triethylsilane. The observed product distribution is readily explained by attack of the intermediate triethylsilyl radical on the solvent. The reaction of **12** with chlorotriethylsilane to give **24** was confirmed independently. Hence, the foregoing results are clearly in favor of a free-radical decay mechanism for **6**.

With other potential hydrogen donors it proved difficult to separate the free-radical process from a probable nucleophilic attack of the substrates on the peroxide **6**. The sensitivity of **6** toward nucleophilic attack is indicated by the fact that the addition of methanol to a $CDCl_3$ solution of **6** caused a ca. ten times faster decay, yielding **12** (66%) and the methyl esters **25** (7%) and **26** (10%).

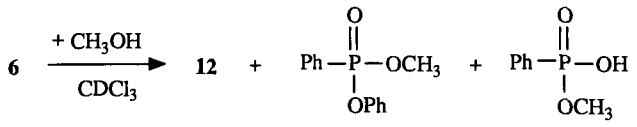

25 **26**

The decay of **6** in $CDCl_3$ was even more strongly accelerated by added phenol. Here, complete destruction of the peroxide occurred within less than ten minutes. Besides **12** (65%) only one product was formed in a considerable amount (30%), which somewhat surprisingly was identified by its ^{13}C-NMR spectrum to be the *ortho*-hydroxylated compound **27**.

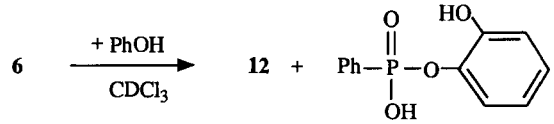

27

Photochemical Decomposition of 6

The photochemically induced decomposition of **6** in $CDCl_3$, CD_3CN, or benzene solution occurred much faster than the thermal reaction but led to very similar products (Figure 2c; see Table 6). For example, UV irradiation at 25°C of 0.11 M solutions of **6** in $CDCl_3$ led to some 57% conversion of the peroxide after 10 minutes, giving an intensely yellow, turbid solution. In all solvents employed, acid **12** was found to be the main product. As indicated by their resonances in the range of $\delta = 16-18$ in the ^{31}P-NMR spectra, the same side products, *viz.* **21**–**23**, as in the thermal experiments were formed. Likewise, the [D_6]DMSO solutions of the precipitates formed on prolonged irradiation gave ^1H-, ^{31}P-, and ^{13}C-NMR spectra showing the signals of the same compounds as found in the thermal reaction.

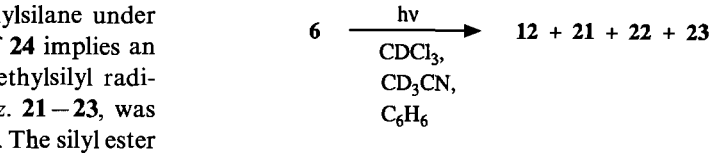

The close similarity of the product patterns from the thermally and the photolytically initiated decomposition of peroxide **6** provides ample evidence that under both conditions a free radical mechanism is followed. This view is again supported by the outcome of the experiments where **6** was photolyzed in the presence of triethylsilane, 1,4-cyclohexadiene, or methanol, respectively (see Experimental).

Laser Flash Photolysis Experiments

Laser Flash Photolysis of 5

When deoxygenated $8 \cdot 10^{-4}$ M solutions of peroxide **5** in acetonitrile were subjected to 248-nm LFP at 20°C, a weak broad absorption in the 400–800 nm range (λ_{max} ca. 580 nm) and sharper, more intense bands between 250 and 350 nm (λ_{max} = 325 nm) were produced within the width of the laser pulse (ca. 20 ns) (Figure 3). The "580-nm" band appeared to be very short-lived; it decayed completely within ca. 60 ns [$k^{580\,nm} = (9.9 \pm 0.3) \cdot 10^7\ s^{-1}$], whereas the decay of the "325-nm" absorption followed a second-order rate law with a much longer lifetime of ca. 2.1 μs [$k/\varepsilon d = (1.7 \pm 0.3) \cdot 10^7\ s^{-1}$] (Figure 4). In the presence of dissolved oxygen the "580-nm" band was not affected, but the lifetime of the short-wavelength bands was strongly reduced, and new bands at $\lambda < 300$ nm (λ_{max} ca. 260 and 280 nm) were observed[13]. We assign the "580-nm" absorption in the visible region to the oxygen-centered radical **7** because of the following reasons: (i) its similarity in shape and wavelength range to other X=O-conjugated oxyl radicals, viz. **2**[2] and the carbonyloxyls[1], (ii) its extremely short lifetime, which renders **7** to be a highly reactive species, and (iii) the fact that this band is not "quenched" by molecular oxygen, as expected for an oxygen-entered radical[1–3]. The

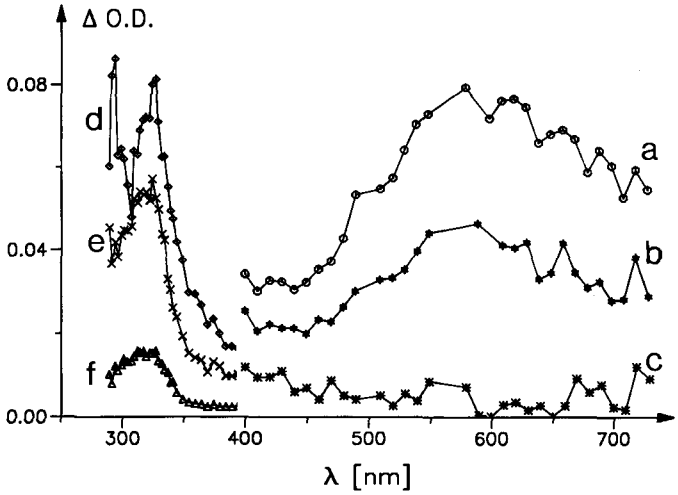

Fig. 3. Transient UV/Vis spectra (20°C) observed after 248-nm LFP of $8 \cdot 10^{-4}$ M solutions of **5** in CD_3CN. (a) 10 ns, (b) 30 ns, (c) 100 ns after the laser flash in oxygen-saturated solution; (d) 100 ns, (e) 1 μs, (f) 10 μs after the laser flash in argon-saturated solution

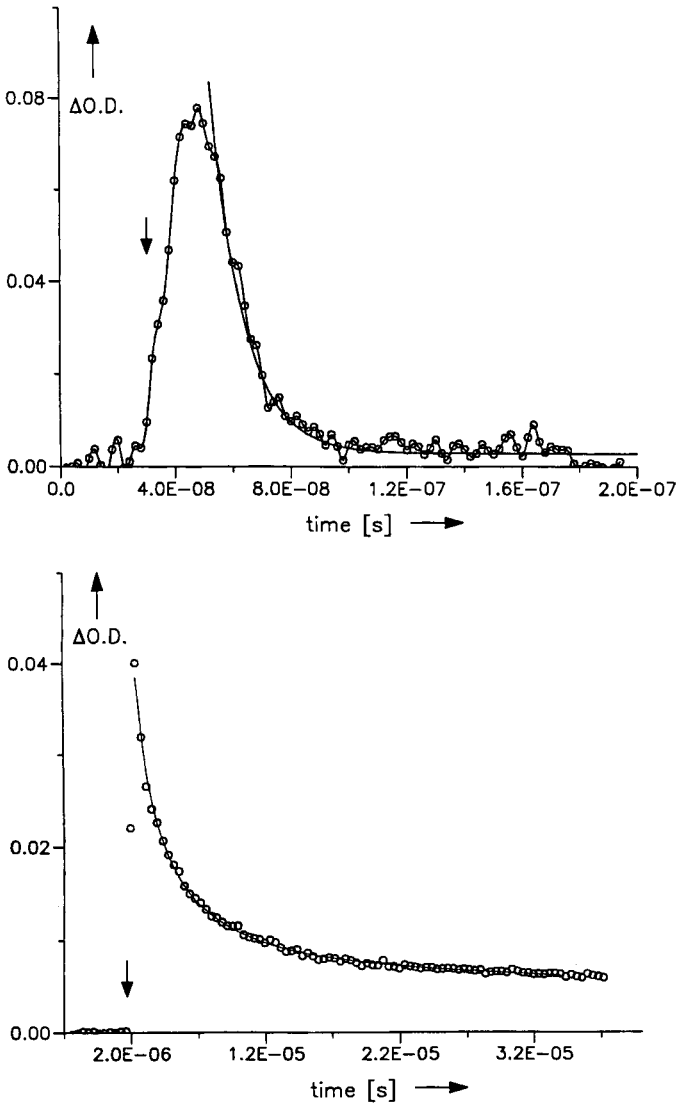

Fig. 4. Time profiles of the absorptions at 550 (top) and 325 nm (bottom) of the LFP spectra shown in Figure 3. Arrows mark the position of the laser pulse. Contiguous lines are the fitted theoretical curves for a first- (top) and second-order (bottom) rate law

fast reaction with oxygen as well as the second-order decay process certainly identify the short-wavelength bands (<340 nm) as being due to carbon-centered radicals, thus reflecting possible intramolecular hydrogen transfer in **7**, intermolecular hydrogen abstraction from the precursor and the solvent, and addition to the phenyl groups[14] of the peroxide. Such reactions are supported by the above NMR product studies and correspond to the release of highly reactive radicals, viz. **7**.

Laser Flash Photolysis of 6

The 248-nm LFP of deoxygenated $4 \cdot 10^{-4}$ M solutions of **6** in CH_3CN at 20°C yielded within the pulse width of the laser flash transient absorption spectra (Figure 5), characterized by a fairly narrow, intense band at $\lambda_{max} = 280 \pm 2$ nm and a broad, less intense absorption with ill-defined maxima at ca. 390 and 410 nm. The intensity of the latter

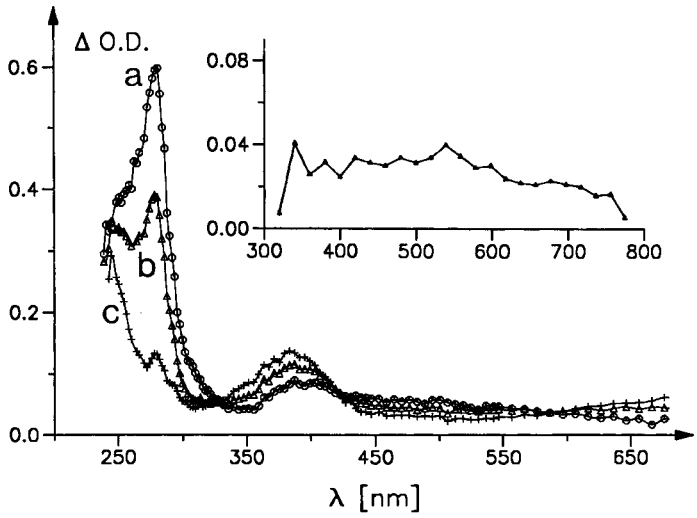

Fig. 5. Transient UV/Vis spectra (20°C) recorded (a) 270 ns, (b) 1.5 μs, (c) 13 μs after 248-nm LFP of a $4 \cdot 10^{-4}$ M solution of **6** in CD_3CN. Inset: Spectrum recorded 16 ns after 308-nm LFP of **6** ($1 \cdot 10^{-2}$ M) in CD_3CN

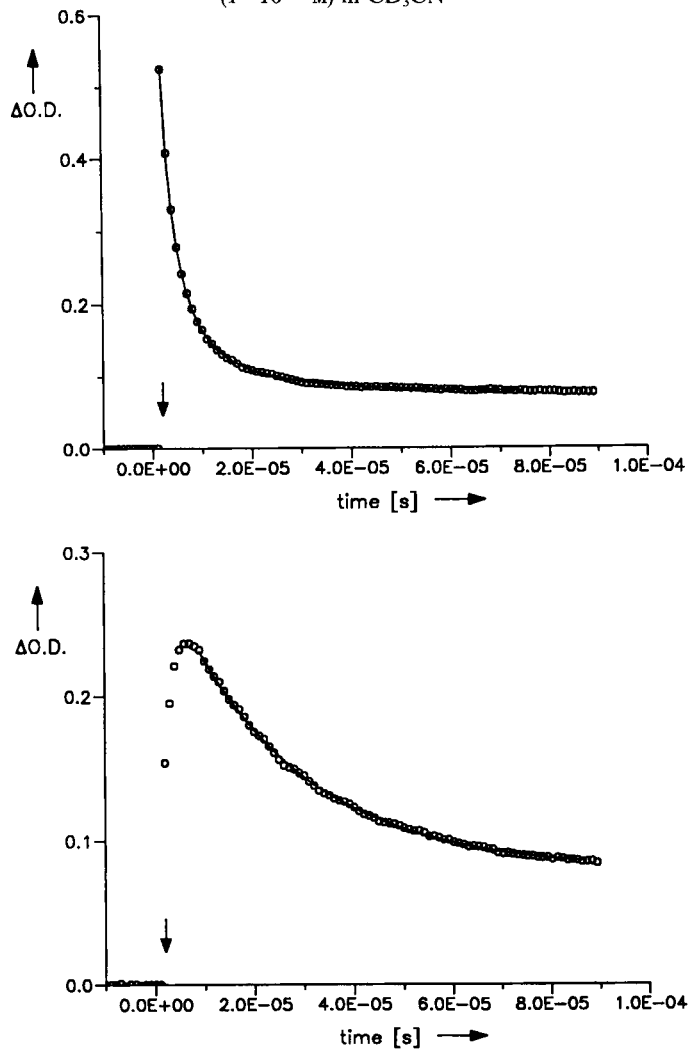

Fig. 6. Time profiles of the absorptions at 288 nm (top) and 390 nm (bottom) of the LFP spectra shown in Figure 5. Arrows mark the position of the laser pulse. Contiguous lines are the fitted theoretical curves for second-order (top; see text) and first-order (bottom) rate laws

band decreased continuously from 410 to ca. 700 nm. Shoulders were detected at 255, 270, and 310 nm. The decay of these absorptions (half-life ca. 4 μs) neither followed a clean first- nor a clean second-order rate law. Below 280 nm the decay profiles were increasingly obscured by the growth of persistent absorptions, which we attribute to the aromatic transitions of some reaction products. In the wavelength range from 285 to 310 nm the absorbance vs. time profiles were perfectly fitted to a superposition of a decaying and a growing, less intense transient species both reacting by a second-order process with average rate constants of $k_d/\varepsilon d = (4.3 \pm 1.2) \cdot 10^5\ s^{-1}$ and $k_g/\varepsilon d = (4.6 \pm 1.1) \cdot 10^5\ s^{-1}$, respectively (Figure 6). The presence of second-order processes also became evident by an approximately linear dependence of the decay rates on the concentration ($4.4 \cdot 10^{-4}$ to $3.3 \cdot 10^{-5}$ M) of the starting peroxide as well as on the incident laser power. The decay of the primary absorptions was accompanied by the growth, with the same rate, of the above mentioned absorptions at $\lambda < 280$ nm and transient absorptions at 390 and 600–800 nm (Figure 5). A direct kinetic relationship between the first-formed and the secondary transient species is suggested by isosbestic points at 330, 430, and 590 nm. The secondary absorptions at 390 and 700–800 nm decayed by a "clean" first-order process with identical rate constants of $k_s = (3.0 \pm 0.5) \cdot 10^4\ s^{-1}$, virtually independent of laser dose and peroxide concentration. No noticeable changes of the absorption bands and the decay kinetics of the first-formed as well as the secondary transient species were observed when the LFP experiments were carried out in an oxygen-saturated solution.

LFP at 308 nm of peroxide **6** in CH_3CN ($1.1 \cdot 10^{-2}$ M; 18 °C) gave similar results. A broad, structureless absorption, continuously decreasing from ca. 400 to 700 nm was observed about 16 ns ("instantaneously") after the flash (Figure 5, inset). At the highest time resolution we could achieve with the laser equipment, an instantaneous "jump" of the absorption in the 450-600 nm range was followed by a partial, extremely fast ($k \geq 10^7\ s^{-1}$) decay. Obviously, two transient species were generated simultaneously (i.e. within the laser pulse width of 4 ns), one of which having a maximum at ca. 540 nm and decaying much faster than the other. Within ca. 90 ns after application of the laser flash the growth of fairly strong absorptions at ca. 390 and 700 nm became increasingly evident. The growth of these secondary absorptions obeyed good first-order kinetics with almost identical rate constants of $k^{390\ nm} = (1.5 \pm 0.2) \cdot 10^6\ s^{-1}$ and $k^{700\ nm} = (1.3 \pm 0.1) \cdot 10^6\ s^{-1}$. However, the latter rate constants were slightly dependent on the laser dose, which indicated a contribution of a second-order process.The secondary transient species again decayed by good first-order kinetics with approximately twice the rate constants [($k_s = (5.7 \pm 0.4) \cdot 10^4\ s^{-1}$)] compared to the 248-nm ($4 \cdot 10^{-4}$ M) experiments.

As for radical **7**, we had expected for radical **8** also a highly transient, broad absorption in the visible region[1–3]. The initial absorptions which we observed in the present case, however, did not fulfil such expectations, i.e. obviously different species had been produced by the laser flash. Guided by the results of the NMR spectroscopic product studies (see above) we reasoned that these transient spectra more likely resembled the features known for oxygen-substituted benzene (anisole-type) radical cations[15]. An attractive explanation for the formation of such a species would be the assumption of an intramolecular electron transfer from the phenoxyl group to one of the oxygen atoms carrying the unpaired electron in the initially generated [(phenoxy)-phenylphosphonyl]oxyl radical **8** to give a zwitterionic form **8Z**. The fact that both the primary and the secondary absorptions as well as their kinetics for formation and decay were not significantly affected by dissolved oxygen agrees with the presence of oxygen-centered radicals as well as aromatic radical cations[15,16].

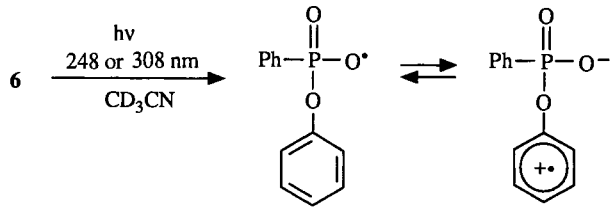

The formation of an anisole-type radical cation, viz. **8Z**, was strongly supported by the transient absorption spectrum which we detected when an CH_3CN solution of methanesulfonyl peroxide **28** was subjected to 248-nm LFP in the presence of phenylphosphonic acid diphenyl ester (**14**) or triphenylphosphate (**29**). The characteristic 450-nm band of the methylsulfonyloxyl radical[3] (**30**) was largely suppressed within ca. 2 μs after the initiating laser flash and replaced by a spectrum stunningly similar to that produced from peroxide **6** (Figure 7). The decay rates of the absorptions at $\lambda = 280$ and 400 nm (half-life ca. 5 μs) were also very similar. Most reasonably, **14** and **29** had been oxidized to their radical cations **31** by the highly electrophilic radical **30**[17] since these spectra could not be observed when **14** or **29** were irradiated in the absence of the sulfonyl peroxide **28**.

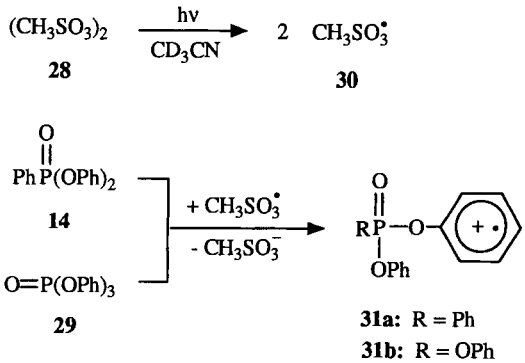

The generation of zwitterion **8Z** would also explain the secondary absorptions produced in the decay of **6** (Figure 4c). The secondary transient spectrum comprised the characteristics of a (substituted) biphenyl radical

cation[5,16,18,19], i.e. a formal dimerization product of **8Z** (see Discussion).

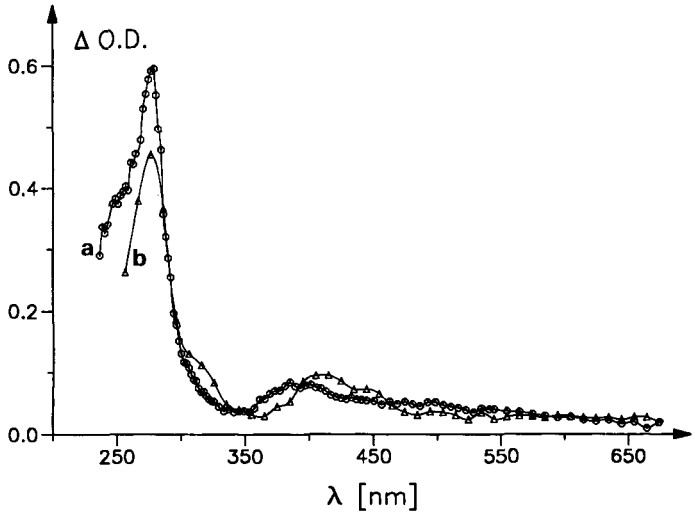

Fig. 7. Transient UV/Vis spectra (20°C) recorded 270 ns after 248-nm LFP of (a) a $4 \cdot 10^{-4}$ M solution of **6** in CD_3CN and (b) a $5 \cdot 10^{-2}$ M solution of **28** in the presence of $1.3 \cdot 10^{-3}$ M **14** in CD_3CN

ESR Measurements

Direct observation by ESR spectroscopy of **7** and **8** would provide unequivocal proof for their formation from peroxides **5** and **6**, respectively, such proof having been achieved with various carbonyloxyl radicals[1b,20]. Unfortunately, no ESR signals could be detected from the photochemical decomposition of $1 \cdot 10^{-2}$ M solutions of **5** in $CFCl_3$ or cyclopropane between −120 and −90°C. Likewise, no spectra could be obtained from **6** in $CHCl_3$ or CH_3CN in the temperature range from −45 to +25°C (here, the low solubility of **6** prohibited the use of cyclopropane or $CFCl_3$, solvents being more suitable for low-temperature ESR studies). Therefore, we turned to the spin-trapping technique in order to transform transient radicals into more persistent and hence, hopefully, identifiable spin adducts.

A variety of spin traps and solvents were tested; in cases where the spectra could be analyzed by simulation (see Table 2) and comparison with literature data[21] they appeared to be in full agreement with the oxygen-centered radicals **7** and **8** being the initial reactive intermediates. The more important results are summarized in the following: From **5** and nitrosodurene (ND) in $CHCl_3$ solution a composite ESR spectrum was slowly produced in the thermal reaction, the dominant spectral feature was identified as being due to the $^{\bullet}CCl_3$ adduct **32**. Other strong signals displayed the spectral characteristics of acylnitroxyl radicals **33**. The intensity of all spectra was dramatically increased by UV photolysis for a few seconds. The $^{\bullet}CCl_3$ adduct **32** was also the major ESR component produced thermally and photochemically from peroxide **6**. Here, an additional spectrum was detected, which we tentatively attributed to the adduct **34** of radical **8** to nitrosodurene on the basis of what little literature data is available on such types of radicals[21].

The fact that $^{\bullet}CCl_3$ radicals were produced under both conditions proves that free-radical species are released which

Table 2. ESR data for some spin adducts produced in the thermal and photochemical decomposition of peroxides **5** and **6** at 20°C

Spin adduct	Solvent	g[b]	Hyperfine splittings [G][a] a_N	a_H	a_{other}
32	$CHCl_3$	2.00718(5)	10.95	–	1.23 ($3\,^{35}Cl$)
	CCl_4	2.0074(1)	10.74		1.35 ($3\,^{35}Cl$)
33	$CHCl_3$	2.00696(3)	7.28	–	–
34	$CHCl_3$	2.0064	15.8[c]	0.47[d]	15.8[c] ($1\,^{31}P$)
35[e]	CCl_4	2.00627(3)	13.33	1.05 (1H)	0.33 ($1\,^{31}P$)
36	C_6H_6	2.00587(3)	10.17	2.80 ($2H_o$)	3.75 ($1\,^{31}P$)
				0.89 ($2H_m$)	
D-36	C_6D_6	2.00598(5)	10.2	–	3.8 ($1\,^{31}P$)
37	$CHCl_3$	2.00681(1)	8.08	–	–
	C_6H_6	2.00679(2)	7.9	–	–
38	C_6H_6	2.00631(3)	13.10	1.00 (1H)	≤0.3
39	$CHCl_3$	2.00626(2)	13.33	1.05 (1H)	0.33 ($1\,^{31}P$)

[a] ±0.03 G. – [b] Errors in the last digit given in parentheses. – [c] Approximate values. – [d] Multiplett of ≥16 lines. – [e] Average values, several very similar radicals.

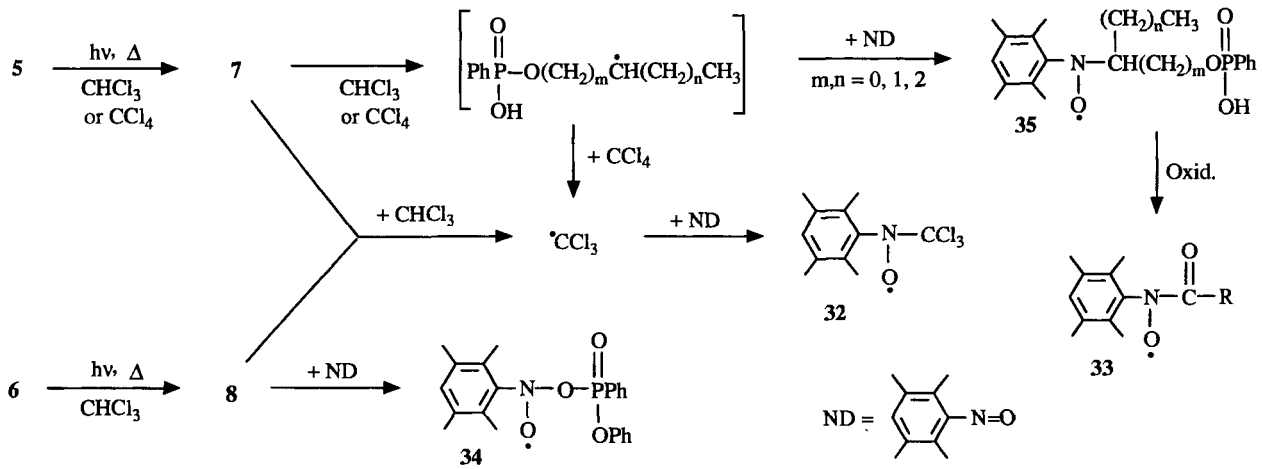

are capable of abstracting hydrogen from $CHCl_3$ at a relatively fast rate. The most likely candidate radicals would certainly be the oxygen-centered radicals **7** and **8**. The appearance of the acylnitroxyls **33** can be attributed to a further oxidation of intermediate alkyl radical adducts **35**, the corresponding alkyl radicals being produced by hydrogen abstraction from the *n*-butyl group.

Hydrogen abstraction by **8** was further indicated by the nitroxyl radical species observed during photolysis of **5** in the presence of nitrosodurene in CCl_4 solution. The detection of the $^{\bullet}CCl_3$ adduct **32** and some other nitroxyls, reasonably attributed to **35**, can be explained in terms of the shown reaction scheme.

In benzene solution the thermal and photochemical decomposition of **5** in the presence of nitrosodurene initially gave a strong spectrum showing the spectral features of a formal adduct (**36**) of a phenyl radical carrying a phosphorus-containing group in the *para*-position. This was unequivocally confirmed by a comparison with the spectral data evaluated from a [D_6]benzene solution (Table 2) where the 3.8-G splitting remained unaffected, thus identifying it to be the hyperfine splitting of the phosphorus atom. The observation of a species like **36** is in line with the expected high reactivity (in addition) of radical **7** towards aromatic substrates.

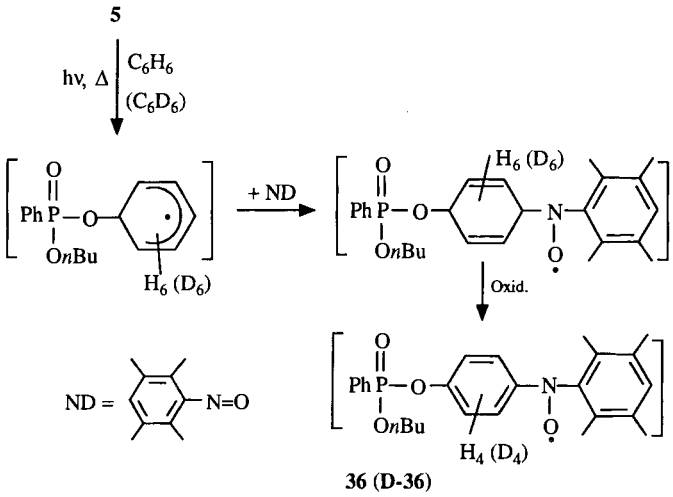

36 (D-36)

With *N-tert*-butylphenylnitrone (PBN) used as spin-trapping agent in $CHCl_3$ solution we observed in the thermal reaction of **5** and **6**, respectively, again a slow build-up of composite ESR spectra whose intensities were dramatically increased by UV photolysis. The spectral parameters of the two most intense features in both spectra were fully consistent with the presence of the acylnitroxyl **37** and adducts **38**, **39** of phosphorus-containing oxyl radicals, viz. **7** and **8**,

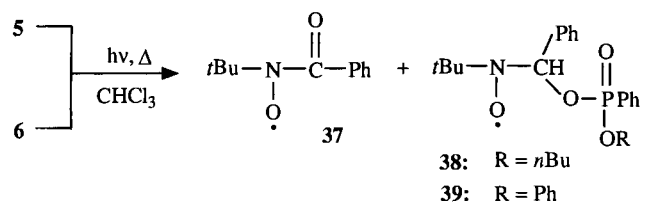

to PBN. Whereas the additional doublet splitting of 0.33 G identifies structure **39** with some certainty, the assignment to **38** must remain somewhat tentative[22].

Discussion

In the present paper we demonstrate that symmetrical peroxides deriving from phenylphosphonic acid monoesters can be prepared by rather simple standard procedures. The failure of previous attempts to synthesize bis(phosphorus) peroxides[4] obviously resulted from the high sensitivity of phosphonoyl peroxides towards nucleophilic attack (e.g. by water), i.e. the choice of unfavorable experimental conditions rather than thermochemical reasons.

The identification of peroxides **5** and **6** turned out to be straightforward by the application of ^{31}P- and ^{13}C-NMR spectroscopy, where due to the chiral phosphorus atoms separate signals for the *meso*- and D,L-diastereomers were detected[23]. We believe that the varying relative yields of the two diastereomers are due to slight variations in the conditions of the preparation, and that they reflect differences in the physical properties. e.g. solubility, of the two diastereomers.

Both peroxides decompose slowly at room termperature in solution and in pure from. The kinetic experiments reveal that in $CDCl_3$ or CD_3CN **6** decays ca. 270 times faster than **5**. This cannot be related to a significantly lower O—O bond strength in **6**. The activation energies for decomposition are (within the error limits) very similar for both peroxides despite the fact that different mechanisms are operating (see below). The fact that the lower thermal stability of **6** predominantly arises from a ca. two times lower *A* factor already reflects the strong influence which is exerted by the type, viz. aryl or alkyl, of the "remote" substituent on the mode of decomposition (see below).

Decomposition of 5

The thermal decomposition of **5** does not produce free (phenylphosphonoyl)oxyl radicals **7** in a noticeable amount. In such case we would have expected a much higher yield of acid **11**, as has been observed in the photochemical experiment (see below). Instead, a smooth formation of the mixed phosphonic phosphoric anhyride **17** was monitored. This reaction would represent a novel rearrangement reaction in which one of the phosphorus-bound phenyl groups migrates formally to one of the peroxy oxygens. This "phosphonyl-phosphoryl rearrangement" has a strong similarity in the formation of the mixed phosphinic phosphonic anhydride **41** in the thermal decay of bis(diphenylphosphinoyl) peroxide (**40**)[2,24], for which a similar activation energy has also been reported[24] (Table 1). Thus, there is no significant influence of the phosphorus-bound substituents on the

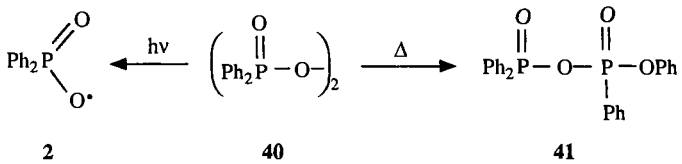

O–O bond strength. The latter "phosphinyl-phosphonyl rearrangement" has been shown to proceed most likely via a nonradical, polar pathway. Therefore, it seems justified to assume for the **5** → **17** rearrangement a similar mechanism.

The ca. four times faster decay of **5** in acetonitrile (Table 3) agrees with a polar contribution. However, such a rate enhancement in the more polar solvent is not as pronounced as expected for an intermediate exhibiting a significantly ionic character. Therefore, the reaction must be assumed to proceed in a largely concerted fashion, probably via either a tight ion pair (as visualized below) or a polarized diradicaloid transition state. It should be noted that the **5** → **17** and **40** → **41** rearrangements represent the phosphorus analoges of the well-known "carboxy-inversion" reaction of diacyl and related peroxides[25], for which similar mechanisms have been reported.

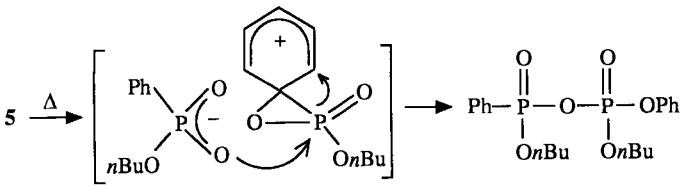

17

Table 3. Rate constants for the thermal decomposition of peroxides **5** and **6**

Peroxide	Solvent	T [°C]	kx10^5 [s^{-1}]	r^2 [a]
5	$CDCl_3$	62	0.48 ± 0.02	0.994
		67	0.86 ± 0.05	0.987
		73	1.55 ± 0.06	0.997
		79	2.41 ± 0.126	0.993
	CCl_4	60	0.37 ± 0.03	0.987
	CD_3CN	62	1.92 ± 0.06	0.999
		22	0.027 ± 0.004	0.983
6	$CDCl_3$	15	0.55 ± 0.01	0.990
		22.5	1.16 ± 0.03	0.996
		28.5	2.95 ± 0.07	0.996
	CD_3CN	28.5	7.20 ± 0.10	0.996

[a] Measure of determination for least-squares fit.

The ESR spin-trap experiments indeed prove that radicals are being produced to some extent in the decay of peroxide **5**, as can be inferred from the detection of the spin adducts reported above. Particularly, the formation of $^{\bullet}CCl_3$ radicals in $CHCl_3$ solution is difficult to explain other than by a "true" free-radical hydrogen abstraction reaction, i.e. some radicals are capable to "leak out" from the otherwise more or less concerted reaction. However, one should be aware that due to the high sensitivity of the ESR method the free-radical reaction may represent only a minor pathway in the thermal decomposition of peroxide **5**. Furthermore, direct nucleophilic attack of the spin-trapping molecules on the peroxide bond, by which radicals **7** would also be released, cannot be excluded.

For the photochemically initiated decomposition of **5** our observations are in agreement with a dominating homolytic O–O bond cleavage to yield the oxygen-centered radical **7**. Hydrogen abstraction to give **11** (Table 5) is by far the most important decay process for this radical and demonstrates its high reactivity towards organic substrates. The extremely short lifetime of the UV/Vis absorption in the 400 to >700 nm range attributed to **7** strongly supports this view. A broad, unstructured absorption in the long-wavelength region can be regarded as a common, characteristic feature of oxyl radicals being in conjugation with a (single) X=O group (X = C or P)[1–3]. This implies that the electronic structure of radical **7** should be very similar to those of the carbonyloxyls[1,20,26] and the (diphenylphosphinoyl)-oxyl radical **2**[2]. ESR spectroscopic[20,26] and theoretical[27] studies have shown that in these radicals the unpaired electron resides almost exclusively in an orbital composed largely of nonbonding oxygen p-type orbitals, oriented more or less in the O=X–O plane. The central atom X provides only a negligible contribution to the SOMO. Although direct ESR observation of **7** (which would give a more direct insight into its electronic structure) has proved not to be possible so far, an electronic structure **A** similar to those commonly accepted for the carbonyloxyls[1b,20,26] can be assumed.

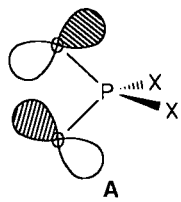

A

From this, further conclusions can be drawn: It would appear that within the series of the phosphorusoxyl radicals $Y_2P(O)O^{\bullet}$ the electronic structure of the upper levels should be more or less the same, no matter if carbon (Y = R) or oxygen substituents (Y = OR') are bound to the central phosphorus atom, i.e. also phosphoryloxyl radicals $[(RO)_2P(O)O^{\bullet}]$ should exhibit comparable spectroscopic and kinetic properties. In nice correspondence with this view, the "entirely" inorganic analoges of our radicals, namely $H_2PO_4^{\bullet}$, $HPO_4^{\bullet -}$, and $PO_4^{\bullet 2-}$, display very similar transient UV/Vis spectra[28] in aqueous solution, i.e. having broad bands with λ_{max} at 520, 510, and 530 nm, respectively. The fact that even negative charges at oxygen (Y = O^-) do not significantly influence the spectroscopic properties of these types of radicals agrees with what has been observed for the sulfonyloxyl radicals[3]. Correspondingly, from the solid-state ESR data[29] of the above phosphoryl species a structure of the SOMO as depicted in **A** also has been deduced. Closely related electronic structures are also predicted by ab-initio and semiempirical PM3 calculations[30].

As a consequence of such an electronic situation the high reactivity of the various X=O-conjugated oxygen-centered radicals should result from a strongly electrophilic character. Therefore, any effect which decreases the *overall* electron density at the oxygens carrying the unpaired spin should lead to an increased reactivity and vice versa. Unfortunately, the weak absorptivity in combination with the rapid "self-quenching" (by intramolecular hydrogen abstraction and reaction with its precursor) of the long-wavelength absorption of **7** prohibited the intented measurement of absolute rate constants for the reaction with organic substrates by the usual method[1,2], i.e. "quenching" of the transient absorption as function of added substrates. Although a quantitative evaluation of the reactivity of **7** was not possible, its short lifetime under the applied conditions renders **7** also to be highly reactive. Thus, π electron donation (if any present) from the *n*-butoxy oxygen to the electron-deficient central phosphorus atom seems to be of minor importance. This view is supported by the similar high reactivity reported for the $H_2PO_4^{\bullet}$ radical[31]. Reasonably reliable measurements of the reactivity of the present class of phosphonoyloxyl radicals have to await the preparation of derivatives carrying substituents which are less prone to attack by oxygen-centerred radicals. Such experiments are currently under way.

Decomposition of 6

The products formed in the decay of peroxide **6** as well as the corresponding transient UV/Vis spectra are in marked contrast to those produced from **5**. No basic difference in the product scheme was observed when the decomposition of **6** was performed by thermal or photolytical initiation. In all experiments acid **12** turned our to be the major component. Thus, a homolytic cleavage of the peroxy bond is strongly suggested to occur under both conditions. The ESR experiments are also in favor of a free-radical mechanism. The transient absorption spectra produced by LFP of peroxide **6**, however, revealed a somewhat more complicated situation. On 248-nm LFP the initially observed spectrum was identified to be due to an oxygen-substituted benzene radical cation rather than to the expected oxygen-centered radical **8**. The relatively high lifetime, the second-order decay process, and the low reactivity towards molecular oxygen[16] are in agreement with such a species[15b,15c,18,19]. We attribute the observed spectrum to the radical cation **8Z**, formally deriving from an intramolecular electron transfer occuring in the oxygen-centered radical **8**[32]. The strong similarity of the initial UV/Vis absorption with the spectrum produced by one-electron oxidation of the esters **14** and **29** with methanesulfonyloxyl radicals **30** provides strong support for this assignment. The formation of **8Z** was further corroborated by identification of the dimeric compounds **22** and (probably) **23** from the reaction mixtures generated by both photolytical and thermal decomposition. Although dimerization has been reported to be a possible decay mode for aromatic radical cations[18] simple C-C coupling of **8Z** followed by double proton shift in the intermediates (Scheme 1, route C; here shown for **42**) to give **22** (and **23**) seems to be of minor importance[33]. The secondary spectrum in Figure 4 appeared to be in full agreement with biphenyl radical cations, in particular a 1,4-dioxy-substituted one[15a,16,18,20]. Thus, **8Z** more reasonably may have decayed by a radical cation substrate reaction[15,16,18], in which the primary adduct **43** (which is not observed)[34] is rapidly converted into the radical cation **44** of compound **22** (path D). A reaction of **8Z** with its

Scheme 1

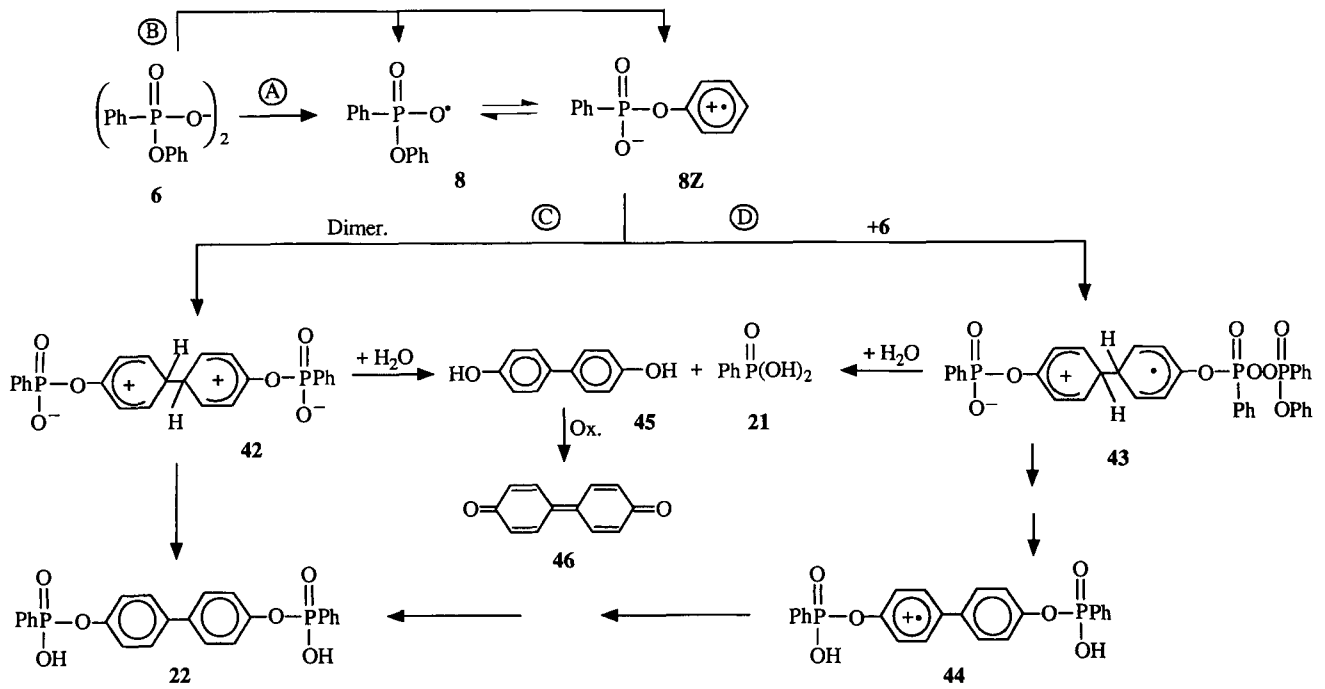

precursor should be of second-order at the low substrate concentration ($4 \cdot 10^{-4}$ M) employed in the 248-nm LFP experiments[35]. The decay process should be shifted towards a pseudo-first-order reaction at higher substrate concentration[18]. This is just what we observed in the 308-nm LFP experiments at ca. 10^{-2} M peroxide concentration (see above). Furthermore, the decay of biphenyl radical cations has been reported to occur by deprotonation with rate constants in the range of 10^3 to 10^5 s^{-1}[16,18,19], covering the range of our data ($k_s = 3-6 \cdot 10^4$ s^{-1}) for the secondary species. Decay of **44** by deprotonation would be in line with the observed products **22** and **23** because the intermediate phenyl-type radicals can be assumed to react predominantly by hydrogen abstraction.

The formation of a dimeric cation intermediate also provides a reasonable explanation for the presence of phenylphosphonic acid (**21**) in the reaction mixtures: The reaction of **43** with traces of water[18] would give **21** and, eventually, 4,4′-dihydroxybiphenyl (**45**). The latter can be further oxidized to give diphenoquinone (**46**). In fact, a characteristic doublet signal at $\delta = 6.73$ ($J = 8.9$ Hz) was observed in the ^{1}H-NMR ([D$_6$]DMSO) spectrum, indicating the presence of small amounts of **45**. Diphenoquinone (**46**) is likely to be responsible for the yellow color of the reaction solutions. Although **46** could not be detected by NMR spectroscopy, it was identified with reasonable certainty by its UV absorption ($\lambda_{max} = 389$ nm) in acetonitrile[36].

An alternative explanation for the formation of **21** would be the assumption of a P–O bond cleavage of **8** or **8Z** to give metaphosphonate **47** and phenoxyl radical **48**. The metaphosphonates are known to react rapidly with nucleophiles[37], i.e. the reaction with traces of water would produce **21**. Recombination of the phenoxyl radicals[38] would lead to 4,4-dihydroxybiphenyl and/or diphenoquinone. We cannot exclude that such processes might be involved to some extent in the the decay of peroxide **6**. However, we could not find any unambiguous spectroscopic evidence for the intermediate formation of phenoxyl radicals[39] nor for the intermediate production of **47**[37].

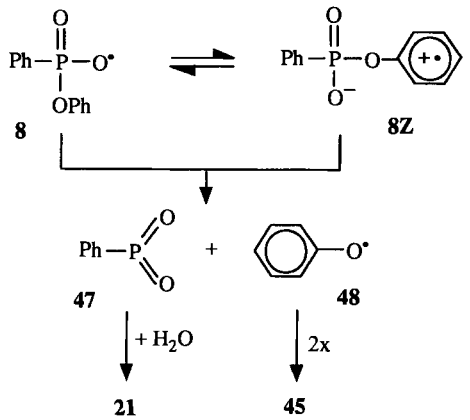

Despite the high intensity of the absorption spectrum assigned to **8Z**, the electron-transfer reaction which leads to this species does not seem to represent the decisive pathway for the formation of the final products. Radical **8** should be still the dominating reactive intermediate since acid **12** has been the major product in all cases. The experimental decay rate of **8Z** then would be governed by the rate of (uphill) back electron transfer from **8Z** to **8**. Absorption bands which could be assigned to the oxygen-centered species **8** were not clearly detected in the 248-nm LFP experiments. However, in the 308-nm LFP experiment (here the incident laser light should have been absorbed mainly by the peroxy bond) a very short-lived absorption around 540-nm has been detected (Figure 5), which might well be attributed to radical **8**. This absorption maximum agrees reasonably well with that observed for the *n*-butoxy-substituted radical **7** (ca. 580 nm) and the inorganic phosphoryl species mentioned above.

With regard to the above results one may envisage several reasonable (however difficult to distinguish) routes for the decomposition of peroxide **6**: (i) electron transfer in the initially generated oxyl radical **8** (path A), very rapidly establishing an equilibrium with **8Z**, (ii) electron transfer already at the stage of the intact peroxide **6**, followed by O–O bond cleavage to give **8** and **8Z** simultaneously (path B), or (iii) even a combination of both routes. Route B would represent the phosporus analogue of an "intramolecular nucleophilic acceleration" of the decomposition of an "...oyl" peroxide[40,41] and is favored to contribute to the overall decay process by the fact that the thermal decomposition of **6** is about 270 times faster than that of peroxide **5** at the same temperature[42].

Conclusively, we have uncovered for a class of long-sought phosphorus-centered peroxides an interesting effect of a "remote" substituent on the mechanism and rate of decay. The high reactivity – as indicated by their short lifetime – of the oxygen-centered radicals **7** and **8** can be related to their strong electrophilic character. The electron-transfer reaction observed for the phenyl-substituted peroxide **6** obviously reflects that property.

We thank Dr. *K. U. Ingold* for valuable discussions, Mr. *H. Bandmann* for recording the NMR spectra, and Drs. *S. Steenken* (MPI, Mülheim) and *J. C. Scaiano* (NRCC, Ottawa) for generous allotment of time on their LFP instruments.

Experimental

^{1}H and ^{13}C NMR (internal standard TMS), ^{31}P-NMR (external standard 85% phosphoric acid): Varian XL 200 and Bruker AMX-300. – IR: Perkin-Elmer 397. – UV: Varian Cary 219. – ESR: Bruker ER-420. – Melting points (uncorrected): Reichert Kofler bench.

Methanesulfonyl peroxide (**28**) was prepared as described[17]. Triphenylphosphate (**29**), phenylphosphonic acid (**21**), phenylphosphonic dichloride, and dichlorophosphoric acid phenyl ester were commercially available (Aldrich).

Dioxybis[(n-butoxy)phenylphosphane oxide] (**5**): To a cold (0°C) solution of sodium peroxide (0.83 g, 10.7 mmol) in water (30 ml) was added with stirring within 30 min a solution of the raw acyl chloride **9** (5 g, 21.5 mmol) in toluene (9 ml). After stirring at 0°C for 2 h the mixture was extracted twice with $CHCl_3$ (25 ml each), and the combined organic layers were concentrated in vacuo to about 15 ml. The solution was dried by passing over neutral alumina (5 × 2 cm), the alumina washed with $CHCl_3$ (20 ml) and the

solvent removed in vacuo from the combined solutions. The light yellow, oily residue (3.15 g; 49%) contained (^{31}P-NMR analysis) 71.2% of **5**, 12.7% of **13**, and 16.1% of **15**. For further purification part (1 g) of the residue was dissolved in $CHCl_3$ (5 ml) and the solution added to cold (−20°C) *n*-pentane (25 ml). After standing for 48 h at −60°C a white solid formed, which we tentatively assigned to be mainly the *meso*-diastereomer[43] of **5**, m.p. 44°C. − ^{31}P NMR ($CDCl_3$): δ = 25.0/25.2 (ratio 87:13). − ^{13}C NMR ($CDCl_3$): δ (*meso*/D,L mixture) = 13.40/13.35 (s), 18.6/18.5 (s), 32.2−32.6 (m, *J* = 2.9 Hz), 67.0−66.7 (m, *J* = 3.6 Hz), 123.9/124.4 (d, *J* = 190.9 Hz), 128.9−128.1 (m), 132.6−132.2 (m), 133.4/133.1 (d, *J* = 3 Hz). − ^{1}H-NMR ($CDCl_3$): δ (*meso*/D,L mixture) = 7.70−7.80 (m, 4H), 7.30−7.50 (m, 6H), 3.90−4.00 (m, 4H), 1.70−1.50 (m, 4H), 1.30−1.50 (m, 4H), 0.85−0.95 (m, 6H). − UV (CD_3CN): λ_{max} (lg ε) = 264 (3.235), 216 (3.420) nm.

$C_{20}H_{28}O_6P_2$ (426.4) Calcd. C 56.34 H 6.62
Found C 55.85 H 7.08

Dioxybis[(phenoxy)phenylphosphane oxide] (**6**): Care had to be taken that during the whole procedure the temperature never exceeded 0°C. To a mixture of sodium carbonate (8.4 g, 40 mmol) in water (100 ml) and 30% hydrogen peroxide (45.2 ml) was slowly added at 0°C a solution of acyl chloride **10** (10 g, 40 mmol) in THF (40 ml) with vigorous stirring. After 4 h the white precipitate was filtered on a glass frit and dissolved in cold (0°C) chloroform (50 ml). Insoluble material was filtered off and the filtrate then dried for 2 h with magnesium sulfate at −77°C. The drying agent was removed by filtration, washed with cold (−20°C) chloroform (20 ml) and then cold (−40°C) pentane (400 ml) was added to the combined filtrates. After 2 h at −77°C the white precipitate was filtered off, dissolved in cold (0°C) chloroform (20 ml) and precipitated by the addition of cold pentane as before. The product was dried in vacuo (10^{-5} mbar) for 1 week at −40°C giving 2.0 g (22%) of white solid, m.p. 118°C (dec.). − ^{31}P NMR ($CDCl_3$): δ = 21.4 (s), 21.2 (s) (intensity ratio varying from 1.7 to 3.2 for material from different runs). − ^{31}P NMR (CD_3CN): δ = 22.3, 22.1. − ^{1}H NMR ($CDCl_3$): δ = 7.00−7.30 (m, 10H), 7.40−7.80 (m, 6H), 7.80−8.00 (m, 4H). − ^{13}C NMR ($CDCl_3$): δ (major isomer) = 120.20 (t, *J* = 2.3 Hz), 123.28 (d, *J* = 191.5 Hz), 125.43 (s), 128.60 (quint., *J* = 6.8 Hz), 129.67 (s), 132.78 (t, *J* = 5.3 Hz), 133.97 (d, *J* = 2.1 Hz), 149.53 (t, *J* = 4.5 Hz). − ^{13}C NMR ($CDCl_3$): δ (minor isomer) = 120.65 (t, *J* = 2.3 Hz), 122.85 (d, *J* = 191.7 Hz), 125.66 (s), 128.50 (quint., *J* = 6.8 Hz), 129.76 (s), 132.66 (t, *J* = 5.3 Hz), 133.74 (d, *J* = 2.1 Hz), 149.3 (t, *J* = 4.5 Hz). − IR (KBr): $\tilde{\nu}$ = 1265 (vs, P=O), 1200 (vs, P−OAr), 790 (vs, br, O−O) cm^{-1}. − UV (CH_3CN): λ_{max} (lg ε) = 266.6 nm (3.156).

$C_{24}H_{20}O_6P_2$ (466.4) Calcd. C 61.81 H 4.32
Found C 61.76 H 4.29

Phenylchlorophosphonic Acid n-Butyl Ester (**9**): Prepared according to ref.[6]; light yellow oil (67%). − ^{31}P NMR ($CDCl_3$): δ = 29.6.

Phenylchlorophosphonic Acid Phenyl Ester (**10**): Synthesized according to ref.[6] (66%), b.p. 138°C (0.08 mbar). − ^{31}P NMR ($CDCl_3$): δ = 26.1 (ref.[7b] 25.1).

Phenylphosphonic Acid Mono-n-butyl Ester (**11**): By refluxing of **9** with water; colorless oil. − ^{31}P NMR ($CDCl_3$): δ = 20.6. − ^{31}P NMR ([D_6]DMSO): δ = 16.2. − ^{13}C NMR ($CDCl_3$): δ = 13.48 (s), 18.60 (s), 32.22 (d, *J* = 6.7 Hz), 65.58 (d, *J* = 6.1 Hz), 128.24 (d, *J* = 15.1 Hz), 128.80 (d, *J* = 193.9 Hz), 131.26 (d, *J* = 9.8 Hz), 132.12 (d, *J* = 3.0 Hz). − ^{1}H NMR ($CDCl_3$): δ = 0.84 (t, *J* = 7.2 Hz, 3H), 1.33 (sext, *J* = 7.2 Hz, 2H), 1.57 (quint, *J* = 8.1 Hz, 2H), 3.97 (q, *J* = 6.6 Hz, 2H), 7.43−7.38 (m, 2H), 7.50−7.47 (m, 1H), 7.82−7.74 (m, 2H).

Phenylphosphonic Acid Monophenyl Ester (**12**): By refluxing of the acyl chloride **10** (1.5 g, 6 mmol) in water (10 ml) for 4 h; 0.82 g (66%), m.p. 84°C (ref.[24] 82°C). − ^{31}P NMR ($CDCl_3$): δ = 17.4−18.5 (concentration-dependent). − ^{31}P NMR (CH_3OH): δ = 15.2. − ^{31}P NMR ([D_6]DMSO): δ = 13.14. − ^{1}H NMR ($CDCl_3$): δ = 7.04−7.26 (m, 5H), 7.41−7.54 (m, 3H), 7.76−7.88 (m, 2H), 11.2 (s, 1H). − ^{13}C NMR ($CDCl_3$): δ = 120.8 (d, *J* = 4.2 Hz), 124.8 (s), 127.8 (d, *J* = 196.2 Hz), 128.4 (d, *J* = 15.6 Hz), 129.5 (s), 131.5 (d, *J* = 10.6 Hz), 132.6 (d, *J* = 3.0 Hz), 150.2 (d, *J* = 7.5 Hz). − ^{13}C NMR ([D_6]DMSO): δ = 120.4 (d, *J* = 4.5 Hz), 124.3 (s), 128.5 (d, *J* = 14.3 Hz), 129.6 (s), 131.3 (d, *J* = 6.8 Hz), 132.1 (d, *J* = 3.0 Hz), 150.8 (d, *J* = 6.8 Hz). − IR (KBr): $\tilde{\nu}$ = 1245 (vs, br, P=O), 1200 (vs, br, P−OAr) cm^{-1}. − UV (CH_3CN): λ_{max} (lg ε) = 264.2 (3.331) nm.

Phenylphosphonic Acid Di-n-butyl Ester (**13**): By reaction of **9** (1.5 g, 6.4 mmol) with *n*-butanol (0.48 h, 6.4 mmol) in the presence of pyridine (0.51 g, 6.4 mmol) in benzene; 1.2 g (76%) of a colorless oil. − ^{31}P NMR ($CDCl_3$): δ = 19.4. − ^{13}C NMR ($CDCl_3$): δ = 13.3 (s), 18.5 (s), 32.2 (d, *J* = 6.6 Hz), 65.5 (q, *J* = 5.6 Hz), 128.1 (d, *J* = 188.7 Hz), 128.2 (d, *J* = 15.1 Hz), 131.5 (d, *J* = 9.8 Hz), 132.1 (d, *J* = 3.0 Hz). − ^{1}H NMR ($CDCl_3$): δ = 7.85−7.78 (m, 2H), 7.60−7.50 (m, 1H), 7.50−7.40 (m, 2H), 4.10−4.00 (m, 4H), 1.70−1.60 (m, 4H), 1.40−1.35 (m, *J* = 7.4 Hz, 4H), 0.91 (t, *J* = 7.4 Hz, 6H).

Phenylphosphonic Acid Diphenyl Ester (**14**): By reaction of **10** with phenol and pyridine in benzene[44], m.p. 70°C (ref.[44] 63.5°C). − ^{31}P NMR ($CDCl_3$): δ = 12.3. − ^{13}C NMR ($CDCl_3$): δ = 120.6 (d, *J* = 4.5 Hz), 125.15 (d, *J* = 0.8 Hz), 126.9 (d, *J* = 193.2 hz), 128.6 (d, *J* = 15.8 Hz), 129.7 (s), 132.3 (d, *J* = 9.8 Hz), 133.2 (d, *J* = 3.0 Hz), 150.4 (d, *J* = 8.3 Hz). − ^{1}H NMR ($CDCl_3$): δ = 7.11−7.34 (m, 10H), 7.49−7.58 (m, 3H), 7.92−8.00 (m, 2H).

Diphenyldiphosphonic Acid Di-n-butyl Ester (**15**): A solution of **11** (0.5 g, 2.3 mmol) in anhydrous diethyl ether (20 ml) was added in one portion to a solution of **9** (0.54, 2.3 mmol) at room temp. Pyridine (0.18 g; 2.3 mmol) in diethyl ether (5 ml) was added slowly with vigrous stirring. After stirring for 2 h the pyridinium salt was filtered off and the solvent removed in vacuo to give a light yellow oil (0.97 g) containing (^{31}P-NMR analysis) 62% of **15**. − ^{31}P NMR ($CDCl_3$): δ (*meso*/D,L mixture, ca. 1:1) = 10.34/10.36. − ^{13}C NMR ($CDCl_3$): δ = 13.33/13.36 (s), 18.37/18.44 (s), 31.90/32.0 (m, *J* ca. 3.3 Hz), 66.57/66.81 (d, *J* = 3.2 Hz), ca. 127.1 (d, *J* ca. 200 Hz), 128.4−128.0 (m), 131.6−131.1 (m), 132.8 (d, *J* = 6.8 Hz). − ^{1}H NMR ($CDCl_3$): δ = 0.82−0.93 (m, 6H), 1.25−1.45 (m, 4H), 1.55−1.75 (m, 4H), 1.40−1.41 (m, 4H), 7.30−7.60 (m, 6H), 7.70−7.95 (m, 4H).

Diphenyldiphosphonic Acid Diphenyl Ester (**16**): Synthesized according to ref.[24], m.p. 95−97°C (ref.[24] 96°C). − ^{31}P NMR ($CDCl_3$): δ = 6.2. − ^{31}P NMR (CD_3CN): δ (*meso*/D,L diastereomeric mixture) = 7.5/7.2. − ^{13}C NMR ($CDCl_3$): δ (*meso*/D,L diastereomeric mixture) = 120.5/120.4 (d/d, *J* = 3.0/3.0 Hz), 125.30/125.26 (s/s), 126.1/126.0 (d,d/d,d, *J* = 204, 3.5/204, 3.5 Hz), 128.3−128.7 (m), 129.6/129.7 (s/s), 132.1 (q, *J* = 5.3 Hz), 133.4 (d, *J* = 1.5 Hz), 149.8 (q, *J* = 3.8 Hz). − ^{1}H NMR ($CDCl_3$): δ = 7.06−7.30 (m, 10H), 7.36−7.60 (m, 6H), 7.80−8.00 (m, 4H).

(Phenylphosphonic Acid Butyl Ester) (Phosphoric Acid Butyl Phenyl Ester) Anhydride (**17**): The synthesis of this compound was attempted by reaction of chlorophosphoric acid butyl phenyl ester with **11** in the presence of pyridine in benzene solution. However, the ^{31}P-NMR ($CDCl_3$) analysis revealed only minor formation of **17**. The observed product spectrum implied a facile disproportionation of **17** to the symmetrical anhydrides **15** and **18**. After a reaction time of 2 h at 20°C the following products were detected:

17 [δ = 10.84/10.63 (d/d, *J* = 7.3/7.3 Hz), −17.91/−18.13 (d/d, *J* = 2.4/2.4 Hz); 11.3%], **18** (δ = −18.52/−18.32; 33.2%), **15** (δ = 10.36/10.35; 36.2%), **19** (δ = −4.78, 4.9%).

Bis(phosphoric Acid Butyl Phenyl Ester) Anhydride (**18**): The reaction of dichlorophosphoric acid phenyl ester (10 g, 47 mmol) with *n*-butanol (3.5 g, 47 mmol) and pyridine (3.7 g, 47 mmol) in benzene (30 ml) gave *chlorophosphoric acid butyl phenyl ester* [10.5 g, 66.5%; ^{31}P NMR ($CDCl_3$): δ = 0.31]. Simultaneous addition of **19** (0.54 g; 2.2 mmol) and pyridine (0.17 g; 2.2 mmol) in benzene (10 ml each) to a benzene solution of this acyl chloride (0.54 g; 2.2 mmol) gave, after standard workup, an oily residue (0.8 g) containing 75.5% of **18**. − ^{31}P NMR ($CDCl_3$): δ (*meso*/D,L mixture) = −18.25/−18.46. − ^{31}P NMR (CD_3CN): δ (*meso*/D,L mixture) = −17.51/−17.60. − ^{13}C NMR ($CDCl_3$): δ = 13.14 (s), 18.09 (s), 31.60/31.60 (s/d, *J* = 7.0 Hz), 69.71/69.65 (d/d, *J* = 7.1/7.3 Hz), 119.75/119.72 (d/d *J* ca. 5.0 Hz), 125.38 (s), 129.48, 149.75 (m, *J* = 6.0 Hz). − ^{1}H NMR ($CDCl_3$): δ = 0.75 (m, 6H), 1.21 (m, 4H), 1.51 (m, 4H), 4.14 (m, 4H), 7.03−7.12 (m, 6H), 7.14−7.22 (m, 4H).

Phosphoric Acid Butyl Phenyl Ester (**19**): By refluxing of chlorophosphoric acid butyl phenyl ester with water; light yellow oil (75.5%). − ^{31}P NMR ($CDCl_3$): δ = −4.26. − ^{13}C NMR ($CDCl_3$): δ = 13.44 (s), 18.47 (s), 31.97 (d, *J* = 7.5 Hz), 68.19 (d, *J* = 6.0 Hz), 120.08 (d, *J* = 5.3 Hz), 124.90 (s), 129.54, 150.58 (d, *J* = 6.8 Hz). − ^{1}H NMR ($CDCl_3$): δ = 0.84 (t, *J* = 7.2 Hz, 3H), 1.31 (sext, *J* = 7.8 Hz, 2H), 1.56 (quint, *J* = 6.9 Hz, 2H), 4.04 (dt, *J* = 6.6 Hz, 2H), 7.07−7.16 (m, 3H), 7.21−7.28 (m, 2H), 12.08 (1H).

Phenylphosphonic Acid Butyl Phenyl Ester (**20**): By reaction of **10** with *n*-butanol and pyridine in benzene; light yellow oil. − ^{31}P NMR ($CDCl_3$): δ = 16.13. − ^{31}P NMR (CD_3CN): δ = 16.32. − ^{13}C NMR (CD_3CN): δ = 13.87 (s), 19.39 (s), 33.05 (d, *J* = 6.8 Hz), 67.35 (d, *J* = 6.0 Hz), 121.48 (d, *J* = 4.5 Hz), 125.87 (d, *J* = 0.8 Hz), 129.93 (d, *J* = 8.3 Hz), 130.70 (s), 132.77 (d, *J* = 9.8 Hz), 133.91 (d, *J* = 3.0 Hz), 150.64 (d, *J* = 6.8 Hz). − ^{1}H NMR (CD_3CN): δ = 0.88 (t, *J* = 7.2 Hz, 3H), 137 (sext, *J* = 7.7 Hz, 2H), 1.64 (m, *J* ca. 7.8 Hz, 2H), 4.15 (dt, *J* = 6.6, 7.5 Hz, 2H), 7.10−7.25 (m, 3H), 7.25−7.40 (m, 2H), 7.45−7.70 (m, 3H), 7.85−7.95 (m, 2H).

Phenylphosphonic Acid (**21**): ^{31}P NMR ($CDCl_3$): δ = 16.6. − ^{31}P NMR ([D_6]DMSO): δ = 13.0. − ^{13}C NMR ([D_6]DMSO): δ = 128.1 (d, *J* = 13.5 Hz), 130.5 (d, *J* = 9.8 Hz), 130.9 (d, *J* = 3.0 Hz), 134.0 (d, *J* = 181.5 Hz).

Bis(phenylphosphonic Acid 4,4′-Biphenyldiyl Ester) (**22**): To a solution of phenylphosphonic dichloride (3.0 g, 15.4 mmol) in benzene (10 ml) were simultaneously added a suspension of 4,4′-dihydroxybiphenyl (**45**) (2.86 g, 15.4 mmol) in benzene (50 ml) and a solution of pyridine (1.22 g, 15.4 mmol) in benzene (25 ml) at 25°C and with vigorous stirring. After stirring for 2 h at 50°C the mixture was filtered and the filtrate concentrated in vacuo. The white residue, which contained (^{31}P-NMR analysis) 47% of the corresponding *P,P′*-dichloride [^{31}P NMR ($CDCl_3$): δ = 26.8], was refluxed with water (100 ml) for 4 h. The mixture was extracted twice with chloroform (25 ml), the solvent removed in vacuo and the white residue dried for 2 d at 50°C/10^{-3} mbar to give 0.9 g (12%) of **22**, m.p. 110°C. − ^{31}P NMR ($CDCl_3$): δ = 17.5−18.6. − ^{31}P NMR ([D_6]DMSO): δ = 13.27. − ^{13}C NMR ([D_6]DMSO): δ = 120.7 (d, *J* = 4.4 Hz), 127.6 (s), 128.5 (d, *J* = 14.6 Hz), 130.3 (d, *J* = 183.2 Hz), 131.25 (d, *J* = 10.3 Hz), 132.1 (d, *J* = 3 Hz), 135.3 (s),

Table 4. Conditions and product distribution (area % of the ^{31}P-NMR signals)[a] for the thermal decomposition of peroxide **5** at 62±1°C

		Products					Peroxide **5** converted
		11	**15**	**17**	**18**	**19**	
Chemical shift δ	(CD_3CN)	20.0	10.7/10.8	11.4/11.2/-17.1/-17.3	-17.6/-17.7	-4.1	25.2 / 25.1
	($CDCl_3$)	20.5	10.3/10.4	10.8/10.6/-17.9/-18.2	-18.3/-18.5	-4.5	25.0 / 24.8
	(CCl_4)	19.4	9.9	10.3/10.2/-17.7/-18.0	-18.4	-4.3	24.3 / 24.25
0.17 M, CD_3CN,	1.2 h	42.8	-	57.2	-	-	3.0
	5.7 h	10.1	19.5	51.2	<0.2	12.0	25.0
	26.7 h	3.7	15.5	68.9	1.0	11.5	83.9
	71 h	5.7	18.3	56.1	3.6	16.3	100
0.37 M, $CDCl_3$,	6.2 h	12.2	38.7	49.2	<0.2	<0.2	5.6
	22 h	23.0	20.7	43.4	<0.2	13.6	20.3
	191 h	18.5	24.4	30.9	3.4	22.8	100
0.26 M, CCl_4,	262 h	34.3	21.2	21.1	0.3	23.1	96.8

[a] Relative to converted peroxide, corrected for initial percentage of compounds **13** and **15**.

150.2 (d, J = 7.0 Hz). – ^{1}H NMR ([D$_6$]DMSO): δ = 7.18 (d, J = 9.6 Hz, 4H), 7.55 (d, m, J = 9.6 Hz, 10H), 7.74–7.86 (m, 4H).

$C_{24}H_{20}O_6P_2$ (466.4) Calcd. C 61.81 H 4.32
Found C 61.61 H 4.63

Bis(phenylphosphonic Acid Ester) **23**: From the reaction mixture of the decomposition of **6**, tentative assignment: ^{13}C NMR ([D$_6$]DMSO): δ = 119.96 (d, J = 4.5 Hz), 120.96 (d, J = 2.7 Hz), 128.58 (d, J = 14.3 Hz), 129.0 (d, J ca. 1 Hz), 130.44 (s), 131.03 (d, J = 9.8 Hz), 131.95 (d, J = 2.3 Hz), 133.18 (s), 147.7 (d, J = 7.5 Hz), 150.1 (d, J = 6.8 Hz).

Phenylphosphonic Acid Phenyl Triethylsilyl Ester (**24**): Equimolar amounts of chlorotriethylsilane and triethylamine were added in an NMR tube to a $CDCl_3$ solution of **11** (10^{-2} M). The ^{31}P-NMR peak of **11** (δ = 17.6) rapidly disappeared and a new peak, assigned to **24**, appeared. – ^{31}P NMR ($CDCl_3$): δ = 6.2 (60.4% rel. intensity). Additional peaks at δ = 11.6 and 6.3 were attributed to the triethylammonium salt of **11** (22.1%) and compound **16** (17.5%), respectively. Attempts to isolate **24** failed.

Phenylphosphonic Acid Methyl Phenyl Ester (**25**): By reaction of **10** (2.0 g, 7.9 mmol) with sodium methanolate (0.43 g, 7.9 mmol) in methanol (5 ml); oil (0.48 g, 25%), b.p. 104–107°C (0.02 mm) (ref.[45] 105–108°C). – ^{31}P NMR ($CDCl_3$): δ = 17.5. – ^{1}H NMR ($CDCl_3$): δ = 3.85 (d, J = 11 Hz, 3H), 6.8–8.2 (m, 10H). A by-product was *phenylphosphonic acid dimethyl ester:* ^{31}P NMR ($CDCl_3$): δ = 22.4. – ^{1}H NMR ($CDCl_3$): δ = 3.75 (d, J = 11 Hz, 6H), 6.8–8.2 (m, 5H).

Phenylphosphonic Acid Methyl Ester (**26**): By reaction of phenylphosphonic dichloride (6.1 g, 31.3 mmol) with methanol (1.0 g, 31.3 mmol) and pyridine (2.4 g, 31.3 mmol) in benzene (20 ml) and refluxing of the raw acyl chloride [^{31}P NMR ($CDCl_3$): δ = 31.8] with water (20 ml); light yellow oil (0.93 g, 17%). – ^{31}P NMR ($CDCl_3$): δ = 20.1. – ^{1}H NMR ($CDCl_3$): δ = 3.68 (d, J = 11.0 Hz, 3H), 7.30–7.55 (m, 3H), 7.65–7.90 (m, 2H), 12.0 (s, 1H) [ref.[46] 3.65 (d, J = 11.0 Hz)].

Phenylphosphonic Acid (2-Hydroxyphenyl) Ester (**27**): Reaction of phenylphosphonic dichloride (1.77 g; 9 mmol) with 1,2-dihydroxybenzene (1.77 g, 9 mmol) and pyridine (0.73 g, 9 mmol) in benzene (150 ml) gave *phenylchlorophosphonic acid (2-hydroxyphenyl)ester* (2.3 g) [colorless oil, ^{31}P NMR ($CDCl_3$): δ = 16.38]. Refluxing with water afforded **27** (oil). – ^{31}P NMR ($CDCl_3$): δ = 14.06. – ^{13}C NMR ([D$_6$]DMSO): δ = 117.56 (s), 119.15 (s), 121.76 (d, J = 3.8 Hz), 128.22 (d, J = 15.1 Hz), 131.33 (d, J = 184.1 Hz), 131.50 (d, J = 9.8 Hz), 131.70 (d, J = 3.0 Hz), 139.38 (d, J = 6.8 Hz), 148.72 (d, J = 4.5 Hz). From a cold benzene solution of the oily product colorless crystals (m.p. 127°C) were slowly formed, which were identified as the pyridinium salt of **27**: ^{31}P NMR ([D$_6$]DMSO): δ = 14.0.

Diphenoquinone (**46**): Synthesized according to ref.[47] – ^{1}H NMR ($CDCl_3$): δ = 6.7 (d, J = 11 Hz), 8.0 (d, J = 11 Hz). – UV (CD_3CN): λ_{max} (lg ε) = 389 (4.651) nm (ref.[36] 394 nm).

Product Studies: Typical experimental conditions are given in Tables 4 and 5. ^{31}P-NMR signals were identified as far as possible by "spiking" with independently synthesized material. Insoluble

Table 5. Conditions and product distribution (area % of the ^{31}P-NMR signals)[a] for the photochemical decomposition of peroxide **5** at 25°C

		Products						Peroxide **5** converted
		11	n.i.[b]	n.i.	n.i.	**20**	n.i.	
Chemical shift δ	(CD_3CN)	20.3	20.2	19.2	18.7	16.7/16.6	15.7	25.2 / 25.1
	($CDCl_3$)	20.7	19.9	19.1	18.7	16.2	16.1	25.0 / 24.8
	(CCl_4)	19.4			18.8	-------15.3[c]-------		24.0
0.17 M, CD_3CN, 45 min		53.2	9.5	10.3	7.9	4.8	1.6	97.8[d]
0.24 M, $CDCl_3$, 45 min		64.8	10.2	5.6	5.6	6.5	1.9	100[e]
0.24 M, $CDCl_3$, 15 min		92.0	-	-	-	-	8.0	24.9
0.13 M, CCl_4, 87 min		80.8	-	-	5.9	------ 3.6 -------		100[f]
0.11 M, CCl_4, 75 min + 1.0 M cyclohexane		93.0	-	-	-	-	5.3	100[g]
0.11 M, CCl_4, 15 min + 1.0 M 1,4-cyclohexadiene		81.6	-	-	5.7	-	-	93.8[h]

[a] Relative to converted peroxide. – [b] Not identified. – [c] Two unresolved peaks. – [d] Additional peaks at δ = 18.3 (7.9%) and 17.6 (1.6%). – [e] Additional peak at δ = 19.6 (5.6%). – [f] Additional peaks at δ = 15.2 (2.0%) and 9.7 (7.7%). – [g] Additional peak at δ = 19.3 (2.3%). – [h] Two additional peaks at δ = 18.0 (6.9%).

products were separated by centrifugation or filtration and dried in vacuo ($<10^{-3}$ mbar).

Thermal decompositions were performed under nitrogen in 5-mm NMR tubes in a thermostated bath. Product distributions and decay kinetics were determined by integration of the ^{31}P-NMR signals. The area percentages given in Tables 4–6 account for >95% of the absolute molar mass balance (from comparison with integrated ^{1}H-NMR spectra). Within the limits of error of integration the ^{31}P-NMR signals of the *meso*- and D,L-diastereomers of **5** and **6**, respectively, decayed at the same rate. Kinetic parameters were obtained from nonlinear least-squares fits of the concentration-time data (Table 3). The Arrhenius activation parameters for the decay of **6** could only be estimated from the rate constants measured between 15 and 28.5 °C. At temperatures above 30 °C the formation of the insoluble products was too rapid to allow a reliable integra-

Table 6. Conditions and product distribution (area % of the ^{31}P-NMR signals)[a] for the thermal and photochemical decomposition of peroxide **6**

		Products					
		12	**22**	**23**[b]	**21**	**16**	Peroxide **6** converted
Chemical shift δ	($CDCl_3$)[c]	17.7	17.5	17.1	16.6	6.2	21.4 / 21.2
	([D_6]DMSO)[d]	13.1	-----13.2 - 13.6----		13.8	6.5	
	(CD_3CN)[d]	17.2	---------- 17.6 ----------				
thermal, 0.063 M, $CDCl_3$, 18.2 h, 22 °C		75.6	8.7	8.7	7.0	-	54
thermal, 0.063 M, $CDCl_3$, 92.6 h, 22 °C		70.4	10.2	8.6	8.6	1.2	93.4
thermal, 0.052 M, $CDCl_3$, 16.8 h, 28.5 °C		63.7	9.2	9.2	9.2	4.1	91.6[e]
		38.1	*42.5*	----- *16.7* ----- [f]			
		57.6	---------- *35.2* ----------			*3.1*[g]	
thermal, 0.066 M, $CDCl_3$, 28 h, 30 °C		65.6	7.2	7.1	8.9	0.6	95.5[h]
		31.5	*18.1*	*14.8*	*35.6*[i]		
thermal, 0.02 M, C_6H_6, 4 d, 22 °C		72.3	10.3	5.2	4.5	-	100[j]
thermal, 0.014 M, CD_3CN, 2.3 h, 28.5 °C		---------- 100 ---------- [k]				-	45.5
thermal, neat, 7 d, 18 °C		78.8	---------3.1----------		0.6	6.8	88.0[l]
photochemical, 0.11 M, $CDCl_3$, 10 min, 23 °C		51.9	14.8	7.4	11.4	8.7	56.7[m]
photochemical, 0.01 M, $CDCl_3$, 11 min, 0 °C		61.9	9.3	10.5	10.5	1.2	95.8[n]
photochemical, 0.014 M, CD_3CN, 3.5 min, 23 °C		84.6	---------- 13.4 ---------- [k]			-	48.8
photochemical, 0.014 M, CD_3CN, 20 min, 23 °C		57.0	19.4	------ 23.5 ----- [k]		-	82.6
		38.3	*47.9*	------ *13.9* ----- [o]			
		53.6	---------- *46.4* ---------- [g]				

[a] Relative to converted peroxide; the percentages given in normal print represent only the dissolved portions of the products. — [b] Tentative assignment. — [c] Average values, actual positions varied by ±0.6 ppm for different solutions. — [d] Average values, ±0.3 ppm. — [e] Additional peak at δ = 9.7 (4.1%). — [f] Relative distribution (in [D_6]DMSO) of the $CDCl_3$-insoluble products (24%). — [g] Calculated overall yields including soluble and insoluble products. — [h] Additional signals at δ = 22.0 (3.0%), 13.4 (1.2%), 12.5 (1.2%), and 9.6 (5.4%). — [i] Relative distribution (in [D_6]DMSO) of the $CDCl_3$-insoluble products (7.2%). — [j] Additional signals at δ = 22.2 (5.8%) and 20.5 (1.9%). — [k] Broad signals, not resolved. — [l] $CDCl_3$-soluble products. — [m] Additional peaks at δ = 21.7 (4.1%) and 13.7 (2.6%). — [n] Additional signals at δ = 22.7 (4.6%) and 13.9 (2.5%). — [o] Relative product distribution (in [D_6]DMSO) of the CD_3CN-insoluble products (18.3%).

tion of the ^{31}P-NMR signals; at lower temperatures crystallization of the peroxide occurred.

For the *photolytic decomposition* deoxygenated solutions of the peroxides were irradiated in 5-mm quartz tubes with the filtered ($\lambda > 360$ nm) light from a 1000-W Hg/Xe lamp.

Decomposition of **5** (0.2 M) in CCl_4 at 62°C in the presence of cyclohexane (1.1 M) led to a complete conversion within 6 d to produce only the ^{31}P-NMR signals of **11** ($\delta = 20.5$; 88.5%) and an unknown, presumably phosphoric acid-derived compound ($\delta = -3.4$; 11.5%).

When 1.1 M 1,4-cyclohexadiene was added to a CCl_4 solution of **5** (0.2 M) decomposition at 62°C occurred much faster (within 45 min), giving mainly **11** (75.8%) and several minor products with ^{31}P-NMR resonances at $\delta = 24.3$ (4.1%), 19.8 (7.4%), 18.8 (4.9%), and 18.3 (4.1%).

Thermal decomposition at 22°C of **6** ($1.3 \cdot 10^{-2}$ M) in CD_3CN solution in the presence of 1 M 1,4-cyclohexadiene gave 80.3% of **12**, 7.2% of **16**, and several minor products in the $\delta = 15-17$ range. The solutions remained colorless, and no formation of insolublc products was observed.

In the presence of 4.6 M methanol, about 86.9% of a 0.11 M solution of **6** in $CDCl_3$ decayed at 25°C within 5 h to give a clear, yellow solution. In the ^{31}P-NMR spectrum ($CDCl_3/CH_3OH$, 4.4:1) the following products were detected: **12** ($\delta = 15.2$; 66.4%), **26** ($\delta = 20.2$, 9.6%), **25** ($\delta = 17.9$; 6.6%), **21**–**23** ($\delta = 14.8$; 9.0%), and several minor products ($\delta = 22.2$, 3.6%; $\delta = 13-14$, 4.8%). In pure methanol as a solvent the only detectable products were **12** (69.3%), **25** (17.5%) and **26** (13.2%).

The addition of phenol (to give a 1 M concentration) to a $6.6 \cdot 10^{-2}$ M solution of **6** in $CDCl_3$ caused a complete dccomposition of **6** within 5 min. The ^{31}P-NMR spectrum showed the presence of **12** (68%) and only one other peak ($\delta = 16.8$; 32%). After removal of the solvent and excess phenol in vacuo (10^{-3} mbar, 30°C) and dissolution of the residue in [D$_6$]DMSO three peaks appeared in the ^{31}P-NMR spectrum due to **12** (64.0%), **27** ($\delta = 14.2$; 30%), and an unidentified product ($\delta = 13.2$; 6%).

A $2 \cdot 10^{-2}$ M $CDCl_3$ solution of **6**, containing 2 M Et_3SiH was converted to about 93.9% after 16 h at 22°C. Products (^{31}P-NMR analysis) were **12** (24.1%), **24** ($\delta = 6.5$; 69.9%), and an unidentified compound with $\delta = 17.9$ (6.0%). Thermolysis of a $2 \cdot 10^{-2}$ M solution of **6** in Et_3SiH-saturated $CDCN_3$ at 24°C gave after 4 h (55.5% conversion) **12** (51.4%), **24** ($\delta = 7.05$; 23.3%), **16** ($\delta = 7.5$ and 7.2; 10.0%), and an unidentified product at $\delta = 20.2$ (6.6%). The percentage of **16** increased slowly on keeping the sample at room temp.; thus, it was probably produced from a slow condensation of ester **24**.

Photolysis at 25°C of a 0.1 M solution of **6** in $CDCl_3$ containing 4.6 M methanol led to 87.5% conversion within 20 min, giving **12** (75.8%), **26** (7.7%), **25** (2.7%), **21**–**23** (8.8%), and several minor products (sum 3.8%).

In the presence of 1 M Et_3SiH a $9 \cdot 10^{-2}$ M solution of **6** in $CDCl_3$ was completely converted after 25 min upon photolysis at 25°C. ^{31}P-NMR analysis of the turbid, yellow solution showed the presence of **12** (56.8%), **21** (8.0%), **22** (8.4%), **23** (5.9%), and **24** (18.4%). Compound **16** was produced in about 44% yield, and the amount of **12** decreased to 25.5% after standing of the reaction mixture in the dark for 8 h. Similarly, photolysis of **6** ($2 \cdot 10^{-2}$ M) in CD_3CN/Et_3SiH (ca. 10:1, v/v) for 7 min (57.4% conversion) gave **12** (57.1%), **24** (14.3%), **16** (14.1%), and **21**–**23** (14.3%).

The photolysis of a $1.3 \cdot 10^{-2}$ M solution of **6** in CD_3CN for 15 min (100% conversion) in the presence of 1 M 1,4-cyclohexadiene gave a colorless solution containing 93.2% of **12** and a byproduct at $\delta = 20.4$ (6.0%).

LFP Measurements: A Lambda Physics EMG 103 MSC excimer laser, operating at 248 nm (KrF, ca. 20 ns pulses) and a Lumonics TE-860-2 excimer laser (308 nm, XeCl, 4 ns pulses) were used. In the 308-nm experiments stationary samples in 7 × 7 mm quartz cells were employed, in the 248-nm experiments the solutions of **5** or **6** in CH_3CN were slowly (ca. 100 ml h^{-1}) pumped through a 4 × 4 mm quartz flow cell. Further details of the equipment and the experimental procedures can be found in refs.[1,48] The kinetic data were evaluated by nonlinear least-squares fitting of the absorbance vs. time data to the appropriate rate laws.

ESR Measurements: The experimental procedures have been described[2,3].

[1] [1a] J. Chateauneuf, J. Lusztyk, K. U. Ingold, *J. Am. Chem. Soc.* **1988**, *110*, 2877–2885, 2886–2893. – [1b] H. G. Korth, J. Chateauneuf, J. Lusztyk, K. U. Ingold, *J. Am. Chem. Soc.* **1988**, *110*, 5929–5931. – [1c] J. Chateauneuf, J. Lusztyk, B. Maillard, K. U. Ingold, *J. Am. Chem. Soc.* **1988**, *110*, 6727–6731. – [1d] H. G. Korth, J. Chateauneuf, J. Lusztyk, K. U. Ingold, *J. Org. Chem.* **1991**, *56*, 2405–2410.

[2] H. G. Korth, J. Lusztyk, K. U. Ingold, *J. Org. Chem.* **1990**, *55*, 624–631, 3966.

[3] H. G. Korth, A. G. Neville, J. Lusztyk, *J. Phys. Chem.* **1990**, *94*, 8835–8839.

[4] E. Bolick, J. Dahlmann, *Methoden Org. Chem. (Houben-Weyl) 4th Ed.*, **1988**, vol. E 13/1, p. 939–949; M. Konieczny, G. Sosnovsky, *Chem. Rev.* **1981**, *81*, 49–77; R. V. Hoffmann in *The Chemistry of Peroxides* (Ed.: S. Patai), Wiley, New York, **1983**, p. 259–277.

[5] There is only one brief report on the preparation of a bisphosphonyl peroxide [MeP(O)(O*n*C$_5$H$_{11}$)O]$_2$: V. I. Barabanov, T. A. Guseva, *Zh. Obshch. Khim.* **1969**, *39*, 1176; engl. 1144.

[6] M. F. Hersman, L. F. Audrieth, *J. Org. Chem.* **1958**, *23*, 1889.

[7] [7a] V. Mark, C. H. Dungan, M. M. Crutchfield, J. R. Van Wazer, *Top. Phosphorus Chem.* **1967**, *5*, 231. – [7b] D. G. Gorenstein, D. O. Shaik in *Phosphorus-31 NMR* (Ed.: D. G. Gorenstein), Academic Press, Orlando, **1984**, ch. 18, p. 549. – [7c] D. G. Gorenstein, *Progr. NMR Spectr.* **1983**, *16*, 1. – [7d] J. C. Tebby in *Phosphorus-31 NMR in Stereochemical Analysis* (Eds.: J. G. Verkade, L. D. Quinn), VCH, Deerfield Beach, **1987**, p. 1.

[8] D. A. Redfield, L. W. Cary, J. H. Nelson, *Inorg. Chem.* **1975**, *14*, 50; see also P. S. Pregosin, R. W. Kunz in *^{31}P- and ^{13}C-NMR of Transition Metal Phosphine Complexes* (Eds.: P. Diehl, E. Fluck, E. Kosfeld), Springer, Berlin, **1977**, p. 66.

[9] H.-O. Kalinowski, S. Berger, S. Braun, *^{13}C-NMR-Spektroskopie*, Thieme, Stuttgart, **1984**.

[10] The sensitivity of **5** towards nucleophiles is clearly demonstrated by the fact that in a water-saturated $CHCl_3$ solution (0.1 M) it decayed completely within 24 h.

[11] In ref.[2] (Table 3) the ^{31}P-NMR resonances at $\delta = 17.8$ and 12.3 were erroneously assigned to anhydride **16** and acid **12**, respectively. The thorough spectral and elemental analyses presented in this paper now allowed an unambiguous assignment. The $\delta = 12.3$ value was actually due to diphenyl phenylphosphonate (**14**). We found that this compound is formed in a considerable amount by refluxing of acid chloride **10** in a water benzene mixture[12], which led to the wrong assignment. The m.p. (70–72°C) given in ref.[12] for acid **12**, therefore, might also actually refer to **14**.

[12] A. Burger, J. Anderson *J. Am. Chem. Soc.* **1957**, *79*, 3575.

[13] Absorption maxima around 270 nm are common for various peroxyl radicals, see: P. Neta, R. E. Huie, *J. Phys. Chem. Ref. Data* **1990**, *19*, 413, and references cited therein.

[14] The 325-nm band might well be due to a cyclohexadienyl-type radical, produced by the addition of **7** to its parent peroxide; the growth of a similar absorption has also been observed in the decay of radical **2**[2]. Alkyl radicals may be responsible for the shorter-wavelength bands, see e.g.: H. R. Wendt, H. E. Hunziker, *J. Chem. Phys.* **1984**, *81*, 717; C. Huggenberger, H. Fischer, *Helv. Chim. Acta* **1981**, *64*, 338.

[15] [15a] T. Shida, *Electronic Absorption Spectra of Radical Ions*, Elsevier, Amsterdam, **1988**. – [15b] P. O'Neill, S. Steenken, D. Schulte-Frohlinde, *J. Phys. Chem.* **1975**, *79*, 953. – [15c] J. Holcman, K. Sehested, *J. Phys. Chem.* **1976**, *80*, 1643–1644.

[16] [16a] K. Sehested, E. J. Hart, *J. Phys. Chem.* **1975**, *79*, 1639–1642. – [16b] J. Mönig, K. D. Asmus, L. W. Robertson, F. Oesch, *J. Chem. Soc., Perkin Trans. 2*, **1986**, 891.
[17] C. J. Myall, D. Pletcher, *J. Chem. Soc.* **1975**, 952; A. G. Neville, H. G. Korth, unpublished.
[18] [18a] A. J. Bard, A. Ledwith, H. J. Shine, *Adv. Phys. Org. Chem.* **1976**, *13*, 155–278. – [18b] O. Hammerich, V. D. Parker, *Adv. Phys. Org. Chem.* **1984**, *20*, 55–190; and references cited therein.
[19] J. K. Kochi, R. T. Tang, T. Bernath, *J. Am. Chem. Soc.* **1973**, *95*, 7114; B. Goodson, G. B. Schuster, *Tetrahedron Lett.* **1986**, *27*, 3123–3126; E. Anklam, K. D. Asmus, L. W. Robertson, *J. Chem. Soc., Perkin Trans 2*, **1989**, 1569–1576.
[20] H. G. Korth, W. Müller, J. Lusztyk, K. U. Ingold, *Angew. Chem.* **1989**, *101*, 186–187; *Angew. Chem. Int. Ed. Engl.* **1989**, *28*, 183–185; H. G. Korth, J. Lusztyk, K. U. Ingold, *J. Chem. Soc., Perkin Trans. 2*, **1990**, 1997–2007.
[21] A. R. Forrester in *Landolt-Börnstein, New Series, Magnetic Properties of Free Radicals* (Eds.: H. Fischer, K. H. Hellwege), Springer, Berlin, **1977**, vol. II/9c1, p. 308; **1987**, vol. II/17d2, p. 49.
[22] The ESR parameters attributed to **38** and **39** are indeed very similar to those of the spin adduct of radical **2** to PBN[2].
[23] For a given composition the relative ratio of the two ^{31}P-NMR peaks was virtually independent of temperature between −20 and +30 °C, proving that no interconversion occurred between the corresponding structure.
[24] R. L. Dannley, K. R. Kabre, *J. Am. Chem. Soc.* **1965**, *87*, 4805–4810; R. L. Dannley, R. L. Waller, R. V. Hoffman, R. F. Hudson, *J. Org. Chem.* **1972**, *37*, 418–421.
[25] S. Oae, K. Fujimori in *The Chemistry of Peroxides* (Ed.: S. Patai), Wiley, New York, **1983**, p. 608; K. Fujimori, S. Oae, *J. Chem. Soc., Perkin Trans 2*, **1989**, 1335.
[26] J. M. McBride, R. A. Merrill, *J. Am. Chem. Soc.* **1980**, *102*, 1723–1725.
[27] See refs.[1a,1d] for leading references.
[28] E. D. Black, E. Hayon, *J. Phys. Chem.* **1970**, *74*, 3199–3203; P. Maruthamuthu, P. Neta, *ibid.* **1978**, *82*, 710–713; see also: G. L. Hug, *Optical Spectra of Nonmetallic Inorganic Species in Aqueous Solution, Natl. Stand. Ref. Data Ser., Natl. Bur. Stand. (U.S.)* **1981**, *69*, 38.
[29] R. Berger, G. Vinand, R. Olazcuaga, M. Zahir, *J. Non-Cryst. Solids* **1983**, *54*, 13. The isotropic *g*-values (2.01–2.02) of these phosphoryl species are indeed in the range of those of the carbonyloxyl radicals[1b,20]; the small ^{31}P hyperfine splittings indicate a negligible spin density at phosphorus; see *Landolt-Börnstein, New Series, Magnetic Properties of Free Radicals* (Eds.: H. Fischer, K. H. Hellwege), Vols. II/9a, II/17a, Springer, Berlin **1977**, **1987**.
[30] Differently to the displayed structure **A**, the calculations predict unequal bond lengths for the two P–O bonds forming the conjugating system; the (largely p-type) SOMO is almost exclusively located at the oxygen atom which is singly bound to the central phosphorus atom; H. G. Korth, W. Sicking, Universität Essen; to be published.
[31] A. B. Ross, P. Neta, *Rate Constants for Reactions of Inorganic Radicals in Aqueous Solution, Natl. Stand. Ref. Data Ser., Natl. Bur. Stand. (U.S.)* **1979**, *65*; P. Neta, R. E. Huie, A. B. Ross, *J. Phys. Chem. Ref. Data* **1988**, *17*, 1027–1285; $H_2PO_4^{\bullet}$ is similar in reactivity to $SO_4^{\bullet-}$, the negatively charged species $HPO_4^{\bullet-}$ and $PO_4^{\bullet 2-}$ show increasingly reduced reactivities.
[32] From their pictoral representation one may be misleaded to regard **8** and **8Z** to be simply mesomeric structures. However, as discussed before, the unpaired electron in **8** resides in an O–P=O in-plane orbital, making resonance interaction with the π system impossible.
[33] Dicationic intermediates like **42** (we are not aware of an unambiguous spectroscopic identification of a dication of that kind) are unlikely to have absorption spectra as observed (Figure 4) and a proton shift is expected to occur much faster than the decay of our secondary transient species.
[34] Broad absorptions in the 500–650-nm range have been reported for such types of radical cation adducts: H. Yamada, K. Kimura, *J. Chem. Phys.* **1969**, *51*, 5733–5734.
[35] If we approximate the unknown molar extinction coefficient of **8Z** at 280 nm by that of the anisole radical cation at the same wavelength ($\varepsilon = 7.24 \cdot 10^3$ l mol^{-1} cm^{-1})[15b,c], then a rate constant of $k_d = 3 \cdot 10^9$ l mol^{-1} s^{-1} can be estimated for the bimolecular decay of **8Z**, i.e. its decay occurs at the diffusion-controlled limit. Correspondingly, the initial concentration of **8Z** produced by a single laser shot is estimated to about $8 \cdot 10^{-5}$ M.
[36] O. B. Lantratova, A. I. Prokof'ev, I. V. Khudyakov, V. A. Kuzmin, I. F. Pokrovskaya, *Nouv. J. Chim.* **1982**, 365. Our measurement of the UV absorption of authentical **46** in CD_3CN (λ_{max} = 389 nm) was in perfect agreement with the absorption of the solutions obtained after decomposition of **6** in CD_3CN. From the optical density (0.005) at 389 nm after decomposition of a $3.7 \cdot 10^{-3}$ M solution of **6** in acetonitrile for 17 h we estimated a concentration of **46** in the range of $1 \cdot 10^{-6}$ M, i.e. too low to be detectable by NMR spectroscopy under the applied conditions.
[37] J. I. G. Cadogan, S. Bracher, I. Gosney, S. Yaslak, *Phosphorus Sulfur* **1983**, *18*, 229; S. Bracher, J. I. G. Cadogan, I. Gosney, S. Yaslak, *J. Chem. Soc., Chem. Commun.* **1983**, 857; *Methoden Org. Chem. (Houben-Weyl). 4th Ed.* **1982**, vol. E 1/1, p. 594, and references cited therein.
[38] D. R. Armstrong, C. Cameron, D. C. Nonhebel, P. G. Perkins, *J. Chem. Soc., Perkin Trans. 2*, **1983**, 563; F. R. Hewgill in *Free Radical Reactions (MTP International Review of Science), Organic Chemistry, Series One*, Butterworth, London, **1973**, p. 167, and references cited therein.
[39] R. H. Schuler, P. Neta, H. Zemel, R. W. Fessenden, *J. Am. Chem. Soc.* **1976**, *98*, 3825; E. P. L. Hunter, M. G. Simic, B. D. Michael, *Rev. Sci. Instrum.* **1985**, *56*, 2199; J. Lind, X. Shen, T. E. Eriksen, G. Merenyi, *J. Am. Chem. Soc.* **1990**, *112*, 479.
[40] Strong rate enhancements by S_N2 or electron-transfer reaction with nucleophiles are well-documented phenomena in the decomposition of diacyl peroxides[41], see: R. Hiatt in *Organic Peroxides Vol. 2*, (Ed.: D. Swern), Wiley, New York, **1972**, ch. 8; B. Plesnicar in *The Chemistry of Peroxides* (Ed.: S. Patai), Wiley, New York, **1983**, p. 546.
[41] For a review on intramolecular electron transfer see: J. C. Martin, *ACS Symp. Ser.* **1978**, *69*, 71–88.
[42] This rate enhancement would also explain why no "phosphonoyl-phosphoryl rearrangement" could be observed for peroxide **6**.
[43] *meso*-Diastereomers normally are less soluble and have higher melting points than the corresponding D,L-diastereomers.
[44] A. Michaelis, F. Kammerer, *Ber. Dtsch. Chem. Ges.* **1875**, *8*, 1306.
[45] T. Otsuki, Y. Okamoto, H. Sakurai, *Synthesis* **1981**, 811.
[46] U. Felcht, M. Regitz, *Chem. Ber.* **1976**, *109*, 3675.
[47] B. R. Brown, A. R. Todd, *J. Chem. Soc.* **1954**, 1280.
[48] [48a] S. Steenken, R. A. McClelland, *J. Am. Chem. Soc.* **1989**, *111*, 4967–4973. – [48b] J. C. Scaiano, *J. Am. Chem. Soc.* **1980**, *102*, 7747.

[111/92]

CAS Registry Numbers

meso-**5**: 142764-21-4 / *rac*-**5**: 142764-38-3 / **6**: 142764-22-5 / 7: 142764-23-6 / **8**: 142764-24-7 / **9**: 18351-25-2 / **10**: 61274-57-5 / **11**: 4098-90-2 / **12**: 2310-87-4 / **13**: 1024-34-6 / **14**: 3049-24-9 / *meso*-**15**: 142764-25-8 / *rac*-**15**: 142764-39-4 / *meso*-**16**: 142764-26-9 / *rac*-**16**: 142764-40-7 / **17**: 142764-27-0 / *meso*-**18**: 142764-28-1 / *rac*-**18**: 142764-41-8 / **19**: 46438-39-5 / **20**: 79905-98-9 / **21**: 1571-33-1 / **22**: 142764-29-2 / **23**: 142764-30-5 / **24**: 142764-31-6 / **25**: 55638-42-1 / **26**: 10088-45-6 / **27**: 7282-99-7 / **32**: 49838-32-6 / **34**: 142764-33-8 / **35** ($m = 1$, $n = 1$): 142764-34-9 / **36**: 142764-35-0 / **D-36**: 142764-32-7 / **37**: 35822-90-3 / **38**: 142764-36-1 / **39**: 142764-37-2 / **40**: 4250-08-2 / **45**: 92-88-6 / **46**: 494-72-4 / BuOH: 71-36-3 / PhOH: 108-95-2 / BuOP(O)(OPh)Cl: 6719-82-0 / $PhP(O)Cl_2$: 824-72-6 / Et_3SiCl: 994-30-9 / 1,2-HOC_6H_4OH: 120-80-9